

Light scalars within the \mathcal{CP} -conserving Aligned-two-Higgs-doublet model

Antonio M. Coutinho,^a Anirban Karan,^a Víctor Miralles,^b Antonio Pich^a

^a*Instituto de Física Corpuscular, Universitat de València – CSIC, Parque Científico, Catedrático José Beltrán 2, E-46980 Paterna, Spain*

^b*Department of Physics and Astronomy, University of Manchester, Oxford Road, Manchester M13 9PL, United Kingdom*

E-mail: antonio.coutinho@ific.uv.es, kanirban@ific.uv.es,
victor.miralles@manchester.ac.uk, antonio.pich@ific.uv.es

ABSTRACT: In this article we study the possibility that neutral and charged scalars lighter than the 125 GeV Higgs boson might exist within the framework of the \mathcal{CP} -conserving Aligned-two-Higgs-doublet model. Depending on which new scalar (scalars) is (are) light, seven different scenarios may be considered. Using the open-source code `HEPfit`, which relies on Bayesian statistics, we perform global fits for all seven light-mass scenarios. The constraints arising from vacuum stability, perturbativity, electroweak precision observables, flavour observables, Higgs signal strengths, and direct-detection results at the LEP and the LHC are taken into account. Reinterpreted data from slepton searches are considered too. It turns out that the seven scenarios contain sizeable regions of their parameter space compatible with all current data. Although not included in the global fits, the possible implications of $(g - 2)_\mu$ are also addressed.

Contents

1	Introduction	1
2	The Aligned-two-Higgs-doublet model	3
3	Constraints	6
4	Fit setup	11
5	Results	13
6	Implications of $(g - 2)_\mu$	21
7	Conclusions	24
A	Direct searches included	27

1 Introduction

The observation of the Higgs boson at the LHC in 2012 [1, 2] firmly cemented the Standard Model (SM) as *the theory of almost everything* [3], our currently accepted picture of elementary particles and their interactions. Still, as the ‘almost’ term denotes, it is widely known that the SM possesses a set of shortcomings that will require the addition of new degrees-of-freedom, which might address all or a few of the issues, while leaving intact what is already known. Among the candidates to build extensions to the SM are scalar fields transforming as doublets of $SU(2)_L$. These are well motivated, if not for anything else, by the fact that fermions have shown Nature’s propensity to bear multiple families of fields: the minimal SM contains a single doublet, but without particular laws prohibiting their existence, it stands to reason that Nature may have produced more than one, following the old adage that “everything not forbidden is compulsory” [4, 5]. Moreover, additional doublets with the same quantum numbers as the SM Higgs leave the tree-level value of the ρ parameter equal to unity [6] and, while extra generations of quarks and leptons are strongly constrained from the Higgs production cross-section at the LHC [7, 8], unitarity-triangle data [9] or Z -boson branching ratios [10], augmenting the SM with scalar doublets circumvents such stringent bounds.

The simplest of such models with multiple doublets is the two-Higgs-doublet model (2HDM) [11, 12], where only one copy is added, and every term that contains the SM Higgs is duplicated. Beyond the three Goldstone bosons, which become the longitudinal polarisations of Z and W^\pm and give mass to these gauge bosons, the 2HDM comes with one charged and three neutral scalars. This enlarged scalar spectrum brings many interesting

possibilities with it, such as new sources of \mathcal{CP} violation [13–20], the smallness of neutrino masses [21, 22], dark matter candidates [23–26], particles with axion-like behaviour [27–32], electroweak baryogenesis [33–39] and the full stability of the vacuum until the Planck scale [40–44] which the SM does not seem able to provide [45–47]. It also comes with its own set of problems, namely the fact that the 2HDM, in its most generic form, introduces tree-level flavour-changing neutral currents (FCNC) that might contribute to certain phenomena beyond what current experimental limits allow. To tackle these pernicious FCNC, the usual implementations of the model impose specific discrete Z_2 symmetries which ensure that each type of right-handed fermions couples with only one of the doublets, thus getting rid of the tree-level flavour-changing interactions altogether [48, 49]. An alternative, less stark solution to the FCNC issue is the alignment of Yukawa couplings in flavour space, so that the diagonalisation of mass terms also trims the non-diagonal elements of the matrices associated with the new neutral scalars. This is the very idea behind the Aligned-two-Higgs-doublet model (A2HDM) [50–52], whose more generic framework adds complexity and offers a richer phenomenology with respect to the Z_2 -symmetric realisations of the model — both at colliders [53–55] and low-energy flavour experiments [56–58]. If complex, the parameters that govern the alignment can be new sources of \mathcal{CP} violation, beyond those usually on offer for 2HDMs: the parameters of the scalar potential not invariant under rephasings, and the Cabibbo–Kobayashi–Maskawa (CKM) matrix [50]. While the alignment condition is scale-dependent and radiative corrections introduce deviations from it at higher loops [59], it has been shown that this proportionality can naturally stem from simple discrete symmetries and be stable under renormalisation-group evolution [60]. Indeed, in general, the flavour violation is minimal [61–64] and FCNC are not only absent at tree-level but also strongly suppressed at higher perturbative orders, ensuring that they do not impact Higgs phenomenology [50–53, 56, 65–68].

Explorations of 2HDMs allowing for scalars lighter than 125 GeV have been published in the literature over the years, most recently in Refs. [69–86]. These recent probes have, for the most part, been focused on possible hints from data for a scalar with a mass around 95 GeV [87–90] and how it could exist within a 2HDM, mainly in its version with a Z_2 symmetry. Concerning the A2HDM, its low-mass region has also been analysed in the past, yet either in scans over limited sections of parameter space or dedicated to tests of a specific set of observables [54–56, 58, 67, 91–97]. A global fit to the A2HDM with no further sources of \mathcal{CP} violation beyond the CKM matrix was first performed in Ref. [98] and subsequently updated in Refs. [99, 100]. Both analyses took a Bayesian approach to statistical inference, powered by the Markov Chain Monte Carlo (MCMC) framework of the publicly available software `HEPfit` [101], yet, in both cases, the spectrum of scalar masses was mostly limited to the heavy scenario, where all new Higgs bosons are assumed to be heavier than the one already observed at the LHC. In this work, we set out to perform, for the first time, a global analysis of the \mathcal{CP} -conserving A2HDM, once more with the aid of `HEPfit`, and following on from preliminary results we have already included in two proceedings papers [102, 103]. With respect to the two previous global fits, this inspection of an enlarged range of masses required the addition of CMS and ATLAS probes of light scalars to the card of LHC data used in the code; additionally, due to their relevance for the regions below 120 GeV

for neutral scalars, and below 100 GeV for charged scalars, we have included the bounds from direct searches at the LEP. Elsewhere, we have brought any colliders' or low-energy experiments' data to their state-of-the-art values, in case they have been updated since the fit of Ref. [99]. We pay particular attention to the anomalous magnetic moment of the muon, which has seen significant developments in recent years. Given the uncertainty that still surrounds its SM value, owing to the existing discrepancies between different methods used in its estimation, we do not include this observable in our main fits. Nevertheless, we devote one section to the examination of the possible influence that $(g-2)_\mu$ could have on our fits, something we also do to the direct searches for supersymmetric (SUSY) particles at the LEP and the LHC that may be reinterpreted as searches for bosons from a generic extended scalar sector.

This paper is organised as follows: in section 2 we present a brief overview of the model; section 3 contains an exposition of the constraints that can be used in fits to the A2HDM; in section 4, we explain the software and statistical setup used to perform our global analyses, whose results are then shown and discussed in section 5; in section 6, we address how different theory predictions of $(g-2)_\mu$ would affect our fits; finally, our main conclusions are given in section 7.

2 The Aligned-two-Higgs-doublet model

The A2HDM is one of the simplest extensions of the SM, as it involves extending the scalar sector by introducing only one additional complex $SU(2)_L$ doublet with a hypercharge of 1/2, exactly like the SM Higgs boson. In general, after electroweak symmetry breaking, the neutral components of both scalar doublets could acquire a vacuum expectation value (vev). However, they can always be redefined through a rotation under the $SU(2)_L \otimes U(1)_Y$ group without loss of generality. This rotation can be chosen such that only one of the two scalars acquires a non-zero vev. This basis is commonly referred to as the Higgs basis, in which the scalar fields after electroweak symmetry breaking can be expressed as

$$\Phi_1 = \frac{1}{\sqrt{2}} \begin{pmatrix} \sqrt{2} G^+ \\ v + S_1 + i G^0 \end{pmatrix}, \quad \Phi_2 = \frac{1}{\sqrt{2}} \begin{pmatrix} \sqrt{2} H^+ \\ S_2 + i S_3 \end{pmatrix}, \quad (2.1)$$

where Φ_1 gets the vev $v = 246$ GeV. The components G^\pm and G^0 can be identified as the Goldstone bosons which provide the masses to the W^\pm and Z bosons. Consequently, the remaining physical spectrum consists of a single charged scalar H^\pm , two \mathcal{CP} -even neutral scalars $S_{1,2}$, and one \mathcal{CP} -odd neutral scalar S_3 . The neutral scalars S_i do not necessarily correspond to the mass eigenstates, since a non-diagonal mass matrix is generated by the most general scalar potential allowed by the SM gauge symmetries:

$$V = \mu_1 \Phi_1^\dagger \Phi_1 + \mu_2 \Phi_2^\dagger \Phi_2 + \left[\mu_3 \Phi_1^\dagger \Phi_2 + \text{h.c.} \right] + \frac{\lambda_1}{2} (\Phi_1^\dagger \Phi_1)^2 + \frac{\lambda_2}{2} (\Phi_2^\dagger \Phi_2)^2 + \lambda_3 (\Phi_1^\dagger \Phi_1)(\Phi_2^\dagger \Phi_2) \\ + \lambda_4 (\Phi_1^\dagger \Phi_2)(\Phi_2^\dagger \Phi_1) + \left[\left(\frac{\lambda_5}{2} \Phi_1^\dagger \Phi_2 + \lambda_6 \Phi_1^\dagger \Phi_1 + \lambda_7 \Phi_2^\dagger \Phi_2 \right) (\Phi_1^\dagger \Phi_2) + \text{h.c.} \right], \quad (2.2)$$

where μ_3 , λ_5 , λ_6 , and λ_7 are complex parameters and the rest are real. Note that there are fewer degrees of freedom than available variables in this equation since the minimisation condition imposes that

$$v^2 = -\frac{2\mu_1}{\lambda_1} = -\frac{2\mu_3}{\lambda_6}. \quad (2.3)$$

Furthermore, by choosing the appropriate phase rotation on Φ_2 one of the complex phases of λ_5 , λ_6 , and λ_7 can be removed, allowing one of these parameters to be taken as real. As such, a total of 11 degrees of freedom can be counted in the scalar sector alone: μ_2 , v , $\lambda_{1,2,3,4}$, $|\lambda_{5,6,7}|$ and the two relative phases between $\lambda_{5,6,7}$.

The mass terms of this potential can be written as

$$V_M = \left(\mu_2 + \frac{1}{2}\lambda_3 v^2 \right) H^+ H^- + \frac{1}{2} \begin{pmatrix} S_1 & S_2 & S_3 \end{pmatrix} \mathcal{M} \begin{pmatrix} S_1 \\ S_2 \\ S_3 \end{pmatrix}, \quad (2.4)$$

with

$$\mathcal{M} = \begin{pmatrix} v^2 \lambda_1 & v^2 \operatorname{Re}(\lambda_6) & -v^2 \operatorname{Im}(\lambda_6) \\ v^2 \operatorname{Re}(\lambda_6) & (\mu_2 + \frac{1}{2}v^2 \lambda_3) + \frac{1}{2}v^2 (\lambda_4 + \operatorname{Re}(\lambda_5)) & -\frac{1}{2}v^2 \operatorname{Im}(\lambda_5) \\ -v^2 \operatorname{Im}(\lambda_6) & -\frac{1}{2}v^2 \operatorname{Im}(\lambda_5) & (\mu_2 + \frac{1}{2}v^2 \lambda_3) + \frac{1}{2}v^2 (\lambda_4 - \operatorname{Re}(\lambda_5)) \end{pmatrix}. \quad (2.5)$$

The physical neutral states h , H , and A would, therefore, be the linear combinations of S_1 , S_2 , and S_3 that diagonalise this mass matrix. In the \mathcal{CP} -conserving limit of the scalar sector, we can take all the $\lambda_{5,6,7}$ as real and the mass matrix becomes block diagonal. Indeed, the mass eigenstates are, in this case, well-defined \mathcal{CP} states: two of them are \mathcal{CP} -even (h , H) whilst the other is \mathcal{CP} -odd (A). In fact, the \mathcal{CP} -odd scalar is just S_3 in this case, since the well-defined \mathcal{CP} states do not mix with each other. In order to diagonalise the mass matrix we only need then to rotate the two \mathcal{CP} -even neutral states,

$$\begin{pmatrix} h \\ H \end{pmatrix} = \begin{pmatrix} \cos \tilde{\alpha} & \sin \tilde{\alpha} \\ -\sin \tilde{\alpha} & \cos \tilde{\alpha} \end{pmatrix} \begin{pmatrix} S_1 \\ S_2 \end{pmatrix}, \quad (2.6)$$

where the scalar h will always be for us the 125 GeV Higgs boson and the scalar H will be the additional new-physics (NP) scalar. From this relation, and taking into account that this rotation diagonalises Eq. (2.5) to the masses of h (M_h) and H (M_H), we obtain the relation

$$\tan \tilde{\alpha} = \frac{M_h^2 - v^2 \lambda_1}{v^2 \lambda_6} = \frac{v^2 \lambda_6}{v^2 \lambda_1 - M_H^2}. \quad (2.7)$$

Using this relation in combination with Eq. (2.4), we can relate some of the parameters of the potential to the physical masses:

$$\mu_2 = M_{H^\pm} - \frac{\lambda_3}{2} v^2, \quad \lambda_1 = \frac{M_h^2 + M_H^2 \tan^2 \tilde{\alpha}}{v^2 (1 + \tan^2 \tilde{\alpha})}, \quad \lambda_4 = \frac{1}{v^2} \left(M_h^2 + M_A^2 - 2M_{H^\pm}^2 + \frac{M_H^2 - M_h^2}{1 + \tan^2 \tilde{\alpha}} \right),$$

$$\lambda_5 = \frac{1}{v^2} \left(\frac{M_H^2 + M_h^2 \tan^2 \tilde{\alpha}}{1 + \tan^2 \tilde{\alpha}} - M_A^2 \right), \quad \lambda_6 = \frac{(M_h^2 - M_H^2) \tan \tilde{\alpha}}{v^2(1 + \tan^2 \tilde{\alpha})}. \quad (2.8)$$

Therefore, we can choose the following nine independent parameters from the scalar sector of the \mathcal{CP} -conserving A2HDM: $\{v, M_h, M_{H^\pm}, M_H, M_A, \tilde{\alpha}, \lambda_2, \lambda_3, \lambda_7\}$, of which the first two have already been precisely measured.

Besides the self-interactions emerging from the scalar potential, the kinetic terms generate interactions of the additional scalars with the gauge bosons. Since S_1 is the only scalar acquiring a vev, it plays the role of the SM Higgs regarding the triple bosonic interactions with two SM gauge bosons. For the mass eigenstates these interactions become

$$g_{hVV} = \cos \tilde{\alpha} g_{hVV}^{SM}, \quad g_{HVV} = -\sin \tilde{\alpha} g_{hVV}^{SM}, \quad g_{AVV} = 0, \quad (2.9)$$

with $VV \equiv W^+W^-, ZZ$.

The gauge symmetries also allow for the emergence of a Yukawa interaction

$$\begin{aligned} -\mathcal{L}_Y = & \left(1 + \frac{S_1}{v}\right) \left\{ \bar{u}_L M_u u_R + \bar{d}_L M_d d_R + \bar{l}_L M_l l_R \right\} \\ & + \frac{1}{v} (S_2 + iS_3) \left\{ \bar{u}_L Y_u u_R + \bar{d}_L Y_d d_R + \bar{l}_L Y_l l_R \right\} \\ & + \frac{\sqrt{2}}{v} H^+ \left\{ \bar{u}_L V Y_d d_R - \bar{u}_R Y_u^\dagger V d_L + \bar{\nu}_L Y_l l_R \right\} + \text{h.c.}, \end{aligned} \quad (2.10)$$

in the Higgs basis of scalars and mass-basis of fermions, where we have omitted the generation indices, and the subscripts L and R refer to the usual left- and right-handed chiral fields. The matrices M_f ($f \equiv u, d, l$) are the diagonal mass matrices of quarks and leptons generated by the vev of Φ_1 , Y_f are the Yukawa matrices coupled to the doublet with zero-vev Φ_2 , and V is the usual CKM matrix. In general, if Y_f are arbitrary 3×3 matrices, these Yukawa interactions would generate FCNC at tree level, which, as mentioned in the introduction, are experimentally highly suppressed. In order to avoid these effects, in the A2HDM an alignment condition between M_f and Y_f is imposed in the flavour space [50, 51] such that

$$Y_u = \varsigma_u^* M_u \quad \text{and} \quad Y_{d,l} = \varsigma_{d,l} M_{d,l}, \quad (2.11)$$

with ς_f , in general, arbitrary complex numbers, yet chosen to be real in our analysis since we assume \mathcal{CP} conservation in the NP throughout this work.

In the scalar mass-eigenstate basis, the interaction with the fermions is given by

$$\begin{aligned} -\mathcal{L}_Y \supset & \left(\frac{\sqrt{2}}{v}\right) H^+ \left[\bar{u} \{ \varsigma_d V M_d \mathcal{P}_R - \varsigma_u M_u^\dagger V \mathcal{P}_L \} d + \varsigma_l \bar{\nu} M_l \mathcal{P}_R l \right] + \text{h.c.} \\ & + \sum_{i,f} \left(\frac{y_f^{\varphi_i^0}}{v}\right) \varphi_i^0 \left[\bar{f} M_f \mathcal{P}_R f \right], \end{aligned} \quad (2.12)$$

with φ_i^0 representing the neutral scalars (h, H , and A) and $\mathcal{P}_{L,R}$ the usual chiral projectors. The couplings $y_f^{\varphi_i^0}$ are related to the parameters defined above by

$$y_u^H = -\sin \tilde{\alpha} + \varsigma_u \cos \tilde{\alpha}, \quad y_u^h = \cos \tilde{\alpha} + \varsigma_u \sin \tilde{\alpha}, \quad y_u^A = -i\varsigma_u,$$

$$y_{d,l}^H = -\sin \tilde{\alpha} + \varsigma_{d,l} \cos \tilde{\alpha}, \quad y_{d,l}^h = \cos \tilde{\alpha} + \varsigma_{d,l} \sin \tilde{\alpha}, \quad y_{d,l}^A = i\varsigma_{d,l}. \quad (2.13)$$

As mentioned before, the A2HDM is a more general theoretical framework that includes as particular cases the usual 2HDMs based on discrete Z_2 symmetries. To recover them we just need to impose $\mu_3 = \lambda_6 = \lambda_7 = 0$ (in the basis where the Z_2 symmetry is enforced), along with

$$\begin{aligned} \text{Type I: } \varsigma_u = \varsigma_d = \varsigma_l = \cot \beta, \quad \text{Type II: } \varsigma_u = -\frac{1}{\varsigma_d} = -\frac{1}{\varsigma_l} = \cot \beta, \quad \text{Inert: } \varsigma_u = \varsigma_d = \varsigma_l = 0, \\ \text{Type X: } \varsigma_u = \varsigma_d = -\frac{1}{\varsigma_l} = \cot \beta, \quad \text{and} \quad \text{Type Y: } \varsigma_u = -\frac{1}{\varsigma_d} = \varsigma_l = \cot \beta. \end{aligned} \quad (2.14)$$

While the imposition of a Z_2 symmetry protects against the appearance of FCNC under renormalisation, this protection is in general absent in the A2HDM because higher-order quantum corrections induce a misalignment between M_f and Y_f . Nevertheless, it is worth noting once more that the symmetries of the A2HDM Yukawa structure impose strong constraints on potential FCNC arising from this misalignment, rendering their effects numerically negligible [50, 51, 56]. Even if exact alignment is assumed at a very high-energy scale, such as the Planck scale, the FCNC effects induced by the renormalisation-group running to low energies remain well below current experimental bounds [52, 53, 65–68].

3 Constraints

In the following, we describe in detail all the different theoretical constraints and experimental observables that we have used in our analysis.

3.1 Vacuum stability

In order to avoid large values of the scalar potential growing in the negative direction, which would make the model unstable, for any given configuration of the scalar fields, the potential must be bounded from below. Various *necessary* conditions on the parameters λ_i for circumventing such large negative potential have recently been discussed in Ref. [104]. The *necessary and sufficient* conditions that ensures the potential to be bounded from below are derived in Refs. [105, 106]. First, one rewrites the scalar potential V (given by Eq. (2.2)) in the Minkowskian *bilinear formalism*:

$$V = -M_\mu \mathbf{r}^\mu + \frac{1}{2} \Lambda^\mu{}_\nu \mathbf{r}^\mu \mathbf{r}^\nu, \quad (3.1)$$

where,

$$\begin{aligned} M_\mu &= \left[-\frac{1}{2}(\mu_1 + \mu_2), -\text{Re} \mu_3, \text{Im} \mu_3, -\frac{1}{2}(\mu_1 - \mu_2) \right], \\ \mathbf{r}^\mu &= \left[|\Phi_1|^2 + |\Phi_2|^2, 2 \text{Re}(\Phi_1^\dagger \Phi_2), 2 \text{Im}(\Phi_1^\dagger \Phi_2), |\Phi_1|^2 - |\Phi_2|^2 \right], \\ \Lambda^\mu{}_\nu &= \frac{1}{2} \begin{bmatrix} \frac{1}{2}(\lambda_1 + \lambda_2) + \lambda_3 & \text{Re}(\lambda_6 + \lambda_7) & -\text{Im}(\lambda_6 + \lambda_7) & \frac{1}{2}(\lambda_1 - \lambda_2) \\ -\text{Re}(\lambda_6 + \lambda_7) & -\lambda_4 - \text{Re} \lambda_5 & \text{Im} \lambda_5 & -\text{Re}(\lambda_6 - \lambda_7) \\ \text{Im}(\lambda_6 + \lambda_7) & \text{Im} \lambda_5 & -\lambda_4 + \text{Re} \lambda_5 & \text{Im}(\lambda_6 - \lambda_7) \\ -\frac{1}{2}(\lambda_1 - \lambda_2) & -\text{Re}(\lambda_6 - \lambda_7) & \text{Im}(\lambda_6 - \lambda_7) & -\frac{1}{2}(\lambda_1 + \lambda_2) + \lambda_3 \end{bmatrix}. \end{aligned} \quad (3.2)$$

Depending on the “*timelike*” (Λ_0) and “*spacelike*” ($\Lambda_{\{1,2,3\}}$) eigenvalues of the mixed-symmetric matrix $\Lambda^\mu{}_\nu$, the *bounded from below* constraint can be recast in three conditions: a) the tensor $\Lambda^{\mu\nu}$ is diagonalisable by a $SO(1,3)$ transformation, b) all the eigenvalues of $\Lambda^\mu{}_\nu$ are real, and c) $\Lambda_0 > 0$ with $\Lambda_0 > \Lambda_{\{1,2,3\}}$, which is equivalent to the statement that *the tensor $\Lambda^{\mu\nu}$ is positive definite in the forward light-cone* [105].

The requirement that the vacuum of the scalar potential should be a stable neutral minimum implies another constraint on the quartic couplings: defining the determinant of the matrix $(\xi \mathbb{I}_4 - \Lambda^\mu{}_\nu)$ as $D = -\prod_{k=0}^3 (\xi - \Lambda_k)$, with the Lagrange multiplier $\xi = \frac{M_{H^\pm}^2}{v^2}$, the existence of a global minimum is ensured if a) $D > 0$, or b) $D < 0$ with $\xi > \Lambda_0$ [106]. Thus, vacuum stability imposes constraints on the mass parameters, quartic couplings, and the mixing angle of the scalars.

3.2 Perturbativity

Perturbative unitarity requires that, at every order of perturbation theory, the scattering amplitudes do not increase monotonically with energy. Thus, imposing this constraint on every $2 \rightarrow 2$ scattering amplitude involving scalars will validate the applicability of the perturbative expansion of the S -matrix by restricting the quartic coupling constants λ_i . Denoting the matrix of tree-level partial wave amplitudes by \mathbf{a}_0 and a_j^0 its corresponding eigenvalues in the j^{th} partial wave, the conditions for *tree-level unitarity* can be expressed as:

$$(a_j^0)^2 \leq \frac{1}{4} \quad \text{with} \quad (\mathbf{a}_0)_{i,f} = \frac{1}{16\pi s} \int_{-s}^0 dt \mathcal{M}_{i \rightarrow f}(s, t). \quad (3.3)$$

However, at tree-level, the S -wave contribution dominates the scattering amplitude at very high energies, and hence it is enough to consider only the $j = 0$ partial wave. The three doubly charged, eight singly-charged, and fourteen neutral two-body scattering states of the scalars can be represented in block-diagonal form as

$$\begin{aligned} \mathbf{a}_0^{++} &= \frac{1}{16\pi} X_{(1,1)}, \quad \mathbf{a}_0^+ = \frac{1}{16\pi} \text{diag} [X_{(0,1)}, X_{(1,0)}, X_{(1,1)}], \\ \mathbf{a}_0^0 &= \frac{1}{16\pi} \text{diag} [X_{(0,0)}, X_{(0,1)}, X_{(1,1)}, X_{(1,1)}], \end{aligned} \quad (3.4)$$

where $X_{(Y,I)}$, representing the scattering amplitudes for states with definite hypercharge and weak isospin, are given by [104, 107]:

$$\begin{aligned} X_{(1,0)} &= \lambda_3 - \lambda_4, \quad X_{(1,1)} = \begin{bmatrix} \lambda_1 & \lambda_5 & \sqrt{2}\lambda_6 \\ \lambda_5^* & \lambda_2 & \sqrt{2}\lambda_7^* \\ \sqrt{2}\lambda_6^* & \sqrt{2}\lambda_7^* & \lambda_3 + \lambda_4 \end{bmatrix}, \\ X_{(0,1)} &= \begin{bmatrix} \lambda_1 & \lambda_4 & \lambda_6 & \lambda_6^* \\ \lambda_4 & \lambda_2 & \lambda_7 & \lambda_7^* \\ \lambda_6^* & \lambda_7^* & \lambda_3 & \lambda_5^* \\ \lambda_6 & \lambda_7 & \lambda_5 & \lambda_3 \end{bmatrix}, \quad X_{(0,0)} = \begin{bmatrix} 3\lambda_1 & 2\lambda_3 + \lambda_4 & 3\lambda_6 & 3\lambda_6^* \\ 2\lambda_3 + \lambda_4 & 3\lambda_2 & 3\lambda_7 & 3\lambda_7^* \\ 3\lambda_6^* & 3\lambda_7^* & \lambda_3 + 2\lambda_4 & 3\lambda_5^* \\ 3\lambda_6 & 3\lambda_7 & 3\lambda_5 & \lambda_3 + 2\lambda_4 \end{bmatrix}. \end{aligned} \quad (3.5)$$

Hence, *tree-level perturbative unitarity* is guaranteed by demanding the eigenvalues (e_i) of all these $X_{(Y,I)}$ matrices to satisfy:

$$|e_i| \leq 8\pi. \quad (3.6)$$

In the \mathcal{CP} -conserving A2HDM the cubic interactions of the neutral and charged scalars are given by

$$V \supset v H^+ H^- \left[(\lambda_3 \cos \tilde{\alpha} + \lambda_7 \sin \tilde{\alpha}) h + (\lambda_7 \cos \tilde{\alpha} - \lambda_3 \sin \tilde{\alpha}) H \right]. \quad (3.7)$$

Therefore, there is a tree-level cubic interaction between the neutral (\mathcal{CP} -even) and charged scalars. These couplings receive a finite vertex correction from the charged scalars themselves [54]:

$$(\lambda_{\varphi_i^0 H^+ H^-})_{\text{eff}} = \lambda_{\varphi_i^0 H^+ H^-} \left[1 + \frac{v^2 \lambda_{\varphi_i^0 H^+ H^-}^2}{16\pi^2 M_{H^\pm}^2} \mathcal{Z} \left(\frac{M_{\varphi_i^0}^2}{M_{H^\pm}^2} \right) \right] \equiv \lambda_{\varphi_i^0 H^+ H^-} (1 + \Delta), \quad (3.8)$$

with

$$\mathcal{Z}(X) = \int_0^1 dy \int_0^{1-y} dz [(y+z)^2 + X(1-y-z-yz)]^{-1}. \quad (3.9)$$

As suggested in Ref. [54], we impose the perturbative constraint $\Delta \leq 0.5$ to guarantee that quantum corrections do not break the perturbative expansion. Thus, like vacuum stability, perturbativity also puts restrictions on the mass parameters, quartic couplings, and the mixing angle of the scalars.

In order to respect perturbativity in the Yukawa sector, we assume the fermionic couplings of the charged scalar to be smaller than unity, which implies: $|\zeta_f| < v/(\sqrt{2} m_f)$.

3.3 Electroweak precision observables

The additional scalar particles modify the vacuum polarisation corrections of the electroweak gauge bosons through their contributions to loop diagrams. These loop effects alter the gauge boson propagators and are parametrised by the oblique parameters (also known as Peskin–Takeuchi parameters [108, 109]) S , T , and U , which encapsulate the deviations caused by NP. In our fit, we only include S and T as observables, assuming U to be negligible — because the contributions to U are highly suppressed in the A2HDM [110]. However, the standard experimental determination of the oblique parameters is obtained from a global electroweak fit [111–113], which also includes the observable $R_b \equiv \Gamma(Z \rightarrow b\bar{b})/\Gamma(Z \rightarrow \text{hadrons})$ [114, 115] as an input. In order to use uncontaminated values for the oblique parameters, we adopt as inputs the results provided in our previous work [99] that were obtained removing R_b from the electroweak fit. For more details, we refer the reader to Appendix B.2 of Ref. [99]. Removing R_b from the oblique-parameter fit is particularly important because we also use R_b as an observable in our analysis, and we need to be sure that we do not double count observables. These observables provide significant restrictions to the splitting of the masses of the new scalars.

3.4 Flavour observables

The presence of new scalar particles coupling to quarks and leptons modifies several precisely measured low-energy observables. Some of these processes are used by the CKMfitter [116] and UTfit [9, 117] collaborations to determine the flavour structure of the SM, providing precise determinations of the CKM matrix. In our fit, we employ the Wolfenstein parametrisation [118] of the CKM matrix, treating its four free inputs as nuisance parameters to which we assign a Gaussian uncertainty. One must mind, though, that the processes used to determine the CKM parameters should not be contaminated by the presence of NP. Even if the UTfit collaboration provides values for the Wolfenstein parameters removing the loop-level processes [119], which are the ones mostly affected by NP, the UTfit fit also includes some tree-level processes that receive contributions from the A2HDM scalars. As such, we proceed as in our previous work [99] and repeat the fit of the Wolfenstein parameters, removing from the fit any process that could be contaminated. For more details on this procedure and the final inputs used, we refer the reader to Appendix B.1 of Ref. [99].

To globally constrain the A2HDM, we take into account all flavour observables that are relevant for \mathcal{CP} -conserving NP. This includes contributions to loop-level processes such as neutral-meson mixing in the B_s system (ΔM_{B_s}) [56, 120], the weak radiative decay $B \rightarrow X_s \gamma$ [56–58, 121–127], and the rare leptonic decay $B_s \rightarrow \mu^+ \mu^-$ [67, 128]. In addition to these loop-induced processes, we also incorporate relevant tree-level transitions. These include leptonic decays of heavy pseudoscalar mesons such as $B \rightarrow \tau \nu$, $D_{(s)} \rightarrow \mu \nu$, and $D_{(s)} \rightarrow \tau \nu$, as well as ratios of leptonic decays of light pseudoscalar mesons, specifically $\Gamma(K \rightarrow \mu \nu)/\Gamma(\pi \rightarrow \mu \nu)$, and the analogous ratio of tau decays $\Gamma(\tau \rightarrow K \nu)/\Gamma(\tau \rightarrow \pi \nu)$ [56]. These flavour observables constrain the maximum allowed values for the alignment parameters, depending on the scalar masses, especially the charged Higgs mass.

3.5 Higgs signal strengths

The introduction of additional scalar fields significantly influences both the production and decay channels of the observed Higgs boson. The one-loop amplitude of $h \rightarrow \gamma \gamma$ is affected by extra contributions arising from the charged scalar. Moreover, the mixing between the \mathcal{CP} -even scalar states alters the couplings between the SM-like Higgs and the weak gauge bosons, as outlined in Eq. (2.9). This modification affects Higgs production via vector-boson fusion (VBF) and its associated production with vector bosons (Vh). Similarly, scalar mixing plays a critical role in the Higgs decay to fermions, as highlighted in Eq. (2.13). This, in turn, has implications for Higgs production mechanisms such as gluon fusion (ggF) and associated production with top quark-antiquark pairs ($t\bar{t}h$).

Since the discovery of the Higgs boson, its properties have been extensively scrutinised at the LHC. In particular, its most relevant production modes (ggF, VBF, Vh , and $t\bar{t}h$) and its subsequent decay channels ($c\bar{c}$, $b\bar{b}$, $\gamma\gamma$, $\mu^+\mu^-$, $\tau^+\tau^-$, W^+W^- , $Z\gamma$, and ZZ) have been measured (or bounded) by the ATLAS and CMS collaborations. Both collaborations provide data parametrised in terms of the Higgs signal strengths, which measure the production cross section in a particular production mode times the branching ratio for a given decay channel, in units of the corresponding SM prediction. In this work, we in-

corporate the complete covariance matrices of signal strength measurements from several key datasets. These include the combined results of ATLAS and CMS at 8 TeV [7], as well as the separate covariance matrices at 13 TeV, provided individually by ATLAS [129] and CMS [130], since a combined analysis is not yet available. Additionally, we include the production and decay channels to charm-quark pairs, which were not accounted for in the aforementioned analyses [131, 132]. These observables put stringent constraints on the mixing angle and the alignment parameters, since the modifications of the Higgs couplings to weak gauge bosons and fermions in the A2HDM depend only on those parameters (see Eqs. (2.9) and (2.13)).

3.6 Direct detection

Additional scalar particles beyond the SM (BSM) have been extensively searched for at different colliders. Due to the different collision energies, the LEP probed Higgsstrahlung-produced scalars up to masses of 120 GeV only, whereas the LHC has performed dedicated searches for both light and heavy scalars. To incorporate these results in our analysis, we compare the theoretically calculated production cross section of a given scalar particle, multiplied by its branching fraction to a particular decay channel, i.e. $\sigma \cdot \mathcal{B}$, to the 95% exclusion limit of the corresponding mode provided by the experimental collaborations. More specifically, we assign a normal distribution (taking only positive values) to the ratio between the theoretical estimate of $\sigma \cdot \mathcal{B}$ and its experimental upper bound, such that its central value becomes 0 and the value 1 is disallowed at 95% probability. We use a linear interpolation method to obtain a continuum from the discrete dataset given by the experiment. Concerning the theoretical predictions of the cross section for various processes, we have made extensive use of the open-source packages MadGraph5_aMC@NLO [133], HIGLU [134] and HDECAY [135], and the tabulated results available in CERN Yellow Reports [136, 137].

All the direct searches for BSM scalars included in our simulation are presented in Appendix A. For the light neutral scalars, we mostly take into account the ATLAS and CMS searches for a resonantly-produced 125 GeV Higgs decaying to two neutral scalars (see Tabs. 3 and 4). Apart from that, we incorporate associated production of light scalars with $t\bar{t}$, $b\bar{b}$, and weak gauge bosons, as given by ATLAS and CMS. The LHC results on a \mathcal{CP} -even neutral scalar decaying to two photons and a \mathcal{CP} -odd neutral scalar decaying to two taus are included too. In addition to the LHC data, we also consider the LEP upper bounds on the pair production of two light neutral scalars and the associated production of one neutral scalar with a Z boson through the Higgsstrahlung process (see Tab. 5).

Regarding the resonant production of a heavy scalar, we consider its decay to the different possible channels: hh , hZ , Z boson associated with another heavy neutral scalar (see Tabs. 6 and 7), two gauge bosons (see Tabs. 8 and 9), and two fermions (see Tabs. 10 and 11), as presented by ATLAS and CMS. Secondary decays from these final states to SM particles are also mentioned in parentheses inside the tables.

Concerning the searches for a light charged Higgs, we implemented the ATLAS and CMS results on a top quark decaying into the H^+b mode (see Tabs. 12 and 13) and the LEP limits on the production of opposite-sign charged scalars through the Z -mediated s-channel

(see Tab. 14). The decay modes of the charged Higgs analysed in these channels are: $\tau^+\nu$, $c\bar{s}$, $\bar{c}b$, and $W^{+*}A$. On the other hand, for a charged scalar heavier than the top quark, we consider the results from ATLAS and CMS, pertaining to its resonant production followed by its decay to $\tau^+\nu$ and $t\bar{b}$ (see Tab. 15).

The presence of light scalars may affect the decay widths, as well as the invisible widths, of several SM particles (like W^\pm , Z , the SM Higgs, and the top quark), which are well measured by experiments. Therefore, these observables put tight constraints on the model parameters. We have taken into account the current upper bounds on the invisible branching fraction of the Higgs boson and the invisible decay widths of the W and Z bosons, as well as the total decay width of the top quark, which are presented in Tab. 16.

3.7 Slepton searches

Many LEP and LHC analyses have been focused on the search for hypothetical SUSY particles. Since the decay of one slepton to a charged lepton and a neutralino resembles the collider signature of a charged Higgs decaying to a charged lepton and a neutrino, one can try to adapt the slepton search data to the 2HDM context [138]. The only difference is that neutrinos are almost massless while neutralinos could have arbitrary large masses. Therefore, the LEP and LHC exclusion plots on slepton masses become relevant for the charged Higgs search at very small neutralino masses. In the absence of an official recasting by the experimental collaborations of their SUSY results into probes of generic scalars, in our analysis we take into account the smuon and stau searches shown in Tab. 17, considering them as reinterpreted searches for the charged Higgs. It is, however, important to mention that only the searches for left-handed sleptons can be reinterpreted as searches for a charged Higgs because both of them have the same $SU(2)_L$ structure. The theoretical estimates for the pair-production cross section of left-handed sleptons (reinterpreted as H^\pm) through the Drell-Yan process at the LEP and the LHC (NLO+NLL) are taken from Refs. [139] and [140–142], respectively.

4 Fit setup

The numerical analysis in this work is performed using the open-source `HEPfit` package [101], which employs a MCMC algorithm implemented via the `Bayesian Analysis Toolkit` [143]. Renowned for its flexibility and computational efficiency, `HEPfit` has been widely utilised for global fits within both the SM [111–113] and various BSM frameworks, including effective field theories [144–154] and specific new physics models [98, 99, 155–161]. For this work, we have significantly modified and extended the existing implementation of the A2HDM in `HEPfit` to enable the exploration of its low-mass regime. Information regarding the exact version of the code used in this analysis can be found in our statement of data availability, at the end of this paper.

Bayesian statistical inference is based on the interpretation of probability as an *update of knowledge*, something that can be conjectured from the expression of Bayes' theorem: the so-called *posterior* distribution of model parameters and observables follows from the statistics derived from all data, denoted as the *likelihood*, times an initial probability density

Priors			
$M_{\phi_{\text{light}}} \in [10 \text{ GeV}, M_h]$		$M_{\phi_{\text{heavy}}} \in [M_h, 700 \text{ GeV}]$	
$\lambda_2 \in [-1, 10]$	$\lambda_3 \in [-1, 10]$		$\lambda_7 \in [-3.5, 3.5]$
$\tilde{\alpha} \in [-0.2, 0.2]$	$\varsigma_u \in [-0.5, 0.5]$	$\varsigma_d \in [-10, 10]$	$\varsigma_l \in [-100, 100]$

Table 1. Priors chosen for the BSM parameters where ϕ_{light} and ϕ_{heavy} denote scalars lighter and heavier than the 125 GeV Higgs, respectively, with $\{\phi_{\text{light}}, \phi_{\text{heavy}}\} \in \{H, A, H^\pm\}$.

function of the full set of parameters, commonly termed *priors*. By sampling from the likelihood distribution, multiplied by one’s choice of *a priori* probability distributions, which can be left flat if no particular initial knowledge — either from experiments or theory computations — exists for a given variable, one gets an updated set of values that reflects how new data has affected one’s *degree of belief*. For a comprehensive exposition of the inferential reasoning that informed the creation of `UTfit` and, subsequently, the development of `HEPfit`, we refer to Refs. [162, 163].

In a Bayesian framework, model comparison between different scenarios can be achieved by evaluating the Information Criterion (IC) [164, 165], defined as

$$\text{IC} = -2 \overline{\log \mathcal{L}} + 4 \sigma_{\log \mathcal{L}}^2, \quad (4.1)$$

where $\overline{\log \mathcal{L}}$ is the average value of the *log-likelihood*, and $\sigma_{\log \mathcal{L}}^2$ its variance. The IC is, thus, characterised by a first term which yields an estimate of the predictive accuracy of the model [166], and a second term that serves as a penalty factor for the number of parameters used in the fit. The preference for a model against another is given according to which one has the smallest IC, with a suggested scale of evidence that can be read from Refs. [167, 168].

4.1 Selection of priors

We now turn to the parameters we use in the fit, and our rationale for the priors that have been chosen for each. The \mathcal{CP} -conserving A2HDM introduces ten additional parameters beyond the SM: three scalar masses (M_A, M_H , and M_{H^\pm}), the mixing angle between the two \mathcal{CP} -even scalars ($\tilde{\alpha}$), three independent quartic couplings (λ_2, λ_3 , and λ_7), and three alignment parameters (ς_u, ς_d , and ς_l). We have taken uniform distributions for the priors, and the ranges of them are chosen wide enough (mostly motivated by the stability and perturbativity bounds) to capture all the aspects of interesting physics signatures relevant for the study of light scalars. While choosing the ranges for the priors, shown in Tab. 1, we have made sure that, after the global fits, there exist no significant statistics in the regions beyond the selected ranges, except for our requirement that forces at least one of the new scalars to be light.

There exists a great freedom regarding the choices of mass parameters for the BSM scalars. As already mentioned, we identify the physical state h as the SM-like Higgs boson with mass $M_h = 125.20$ GeV. The scenario with all the additional scalars heavier than the

Higgs has been well studied in Refs. [98, 99]. In this paper, we examine the possibility of the existence of scalars lighter than M_h . Seven distinct scenarios might appear, corresponding to different scalar mass ranges: 1) three cases with only one BSM scalar lighter than M_h , 2) three cases with two BSM scalars lighter than M_h , and 3) the case with all three BSM scalars lighter than M_h . We have performed global fits for the seven light-scalar scenarios, separately. As can be seen in Tab. 1, we consider the mass of the light scalars to be within the range of 10 GeV to M_h , whereas the heavy scalar masses are taken to be between M_h and 700 GeV. In principle, one could use as priors either the masses or their squares; however, as was already noticed in Ref. [98], the results obtained with the second choice turn out to be more sensitive to the chosen ranges of the priors. We thus restrict ourselves to the choice of linear priors only.

5 Results

Here we show the results of the seven scenarios introduced in Sec. 4, which have been analysed in this work. After performing the fits, and despite imposing strong priors on the masses, we found that all the posterior probabilities of the observables, for all the scenarios, were compatible with the measurements within two standard deviations.¹ An immediate conclusion would be, then, that all scenarios contain a region of the parameter space compatible with all current data. Regarding the goodness of the fits, we found that all of them have similar values of the IC, as shown in Tab. 2, meaning that the seven scenarios have a similar performance, though the cases with only one light neutral scalar perform slightly better. The IC values for the fits involving a single light neutral scalar are, in fact, remarkably close to those obtained from a global analysis that also allows all BSM scalars to be heavy, namely that from Ref. [99]. The marginalised posterior distributions resulting from each fit are also summarised in Tab. 2, with the information on masses presented in their 95% probability ranges, while for the other model parameters we offer the mean value and the standard deviation. In general, since at least one scalar was forced to be light, all scenarios prefer quite small values also for the mixing angle and the Yukawa alignment parameters with the absolute maxima at a 68% probability: $\tilde{\alpha} \lesssim 0.05$ rad, $\varsigma_u \lesssim 0.1$, $\varsigma_u \lesssim 1.7$, and $\varsigma_l \lesssim 42$. However, the precise values for each scenario considered may differ significantly. In the following, we detail the correlations among the different parameters for all scenarios.

5.1 Allowed regions for the model parameters

Scalar potential couplings.- The correlations among the parameters of the potential are summarised in Fig. 1 for all seven scenarios. The coupling λ_2 is only constrained by perturbative unitarity; therefore, its allowed regions are very similar in all scenarios, since they do not depend on the values of the masses. As shown by Eq. (3.7), λ_3 and λ_7 are directly related to the couplings $\lambda_{hH^+H^-}$ and $\lambda_{HH^+H^-}$; thus, they govern the decay of the \mathcal{CP} -even neutral scalars into H^+H^- . Imposing the loop contributions to be smaller than

¹This would not be the case for $(g-2)_\mu$ when using the 2020 white paper prediction but, as explained before, we have not included this observable in our main result.

Marginalised Individual Results				
$M_H \leq M_h$	IC: 84.06	$65 \leq M_H \leq M_h$	$168 \leq M_A \leq 496$	$196 \leq M_{H^\pm} \leq 500$
	$\lambda_2 : 4.969 \pm 1.925$	$\lambda_3 : 3.854 \pm 2.067$	$\lambda_7 : 0.005 \pm 0.382$	
	$\tilde{\alpha} : (0.8 \pm 34.0) \times 10^{-3}$	$\varsigma_u : 0.001 \pm 0.073$	$\varsigma_d : 0.017 \pm 1.716$	$\varsigma_l : -0.325 \pm 20.100$
$M_A \leq M_h$	IC: 83.74	$182 \leq M_H \leq 500$	$69 \leq M_A \leq M_h$	$196 \leq M_{H^\pm} \leq 500$
	$\lambda_2 : 4.609 \pm 1.891$	$\lambda_3 : 3.817 \pm 1.973$	$\lambda_7 : 0.006 \pm 1.164$	
	$\tilde{\alpha} : (-0.8 \pm 42.5) \times 10^{-3}$	$\varsigma_u : 0.003 \pm 0.106$	$\varsigma_d : 0.008 \pm 1.348$	$\varsigma_l : 0.105 \pm 15.380$
$M_{H^\pm} \leq M_h$	IC: 88.48	$M_h \leq M_H \leq 500$	$M_h \leq M_A \leq 440$	$97 \leq M_{H^\pm} \leq M_h$
	$\lambda_2 : 4.342 \pm 2.185$	$\lambda_3 : 0.280 \pm 0.214$	$\lambda_7 : 0.004 \pm 0.873$	
	$\tilde{\alpha} : (-1.7 \pm 41.9) \times 10^{-3}$	$\varsigma_u : 0.0006 \pm 0.0364$	$\varsigma_d : 0.004 \pm 0.706$	$\varsigma_l : 0.528 \pm 34.450$
$M_{H,A} \leq M_h$	IC: 89.48	$89 \leq M_H \leq M_h$	$78 \leq M_A \leq M_h$	$154 \leq M_{H^\pm} \leq 226$
	$\lambda_2 : 4.890 \pm 2.166$	$\lambda_3 : 1.042 \pm 0.5718$	$\lambda_7 : 0.002 \pm 0.362$	
	$\tilde{\alpha} : (-0.6 \pm 47.4) \times 10^{-3}$	$\varsigma_u : 0.002 \pm 0.082$	$\varsigma_d : 0.007 \pm 1.620$	$\varsigma_l : 0.370 \pm 9.574$
$M_{H,H^\pm} \leq M_h$	IC: 89.51	$85 \leq M_H \leq M_h$	$M_h \leq M_A \leq 534$	$95 \leq M_{H^\pm} \leq 120$
	$\lambda_2 : 4.639 \pm 2.208$	$\lambda_3 : 0.254 \pm 0.191$	$\lambda_7 : 0.002 \pm 0.453$	
	$\tilde{\alpha} : (0.2 \pm 38.2) \times 10^{-3}$	$\varsigma_u : -0.0004 \pm 0.0400$	$\varsigma_d : -0.010 \pm 0.656$	$\varsigma_l : -0.603 \pm 41.45$
$M_{A,H^\pm} \leq M_h$	IC: 89.35	$M_h \leq M_H \leq 163$ $\cup 211 \leq M_H \leq 553$	$85 \leq M_A \leq M_h$	$95 \leq M_{H^\pm} \leq 120$
	$\lambda_2 : 4.082 \pm 2.157$	$\lambda_3 : 0.246 \pm 0.192$	$\lambda_7 : -0.005 \pm 0.993$	
	$\tilde{\alpha} : (-0.9 \pm 41.0) \times 10^{-3}$	$\varsigma_u : -0.0004 \pm 0.0402$	$\varsigma_d : 0.001 \pm 0.779$	$\varsigma_l : 0.261 \pm 31.090$
$M_{H,A,H^\pm} \leq M_h$	IC: 89.22	$91 \leq M_H \leq M_h$	$83 \leq M_A \leq M_h$	$95 \leq M_{H^\pm} \leq 122$
	$\lambda_2 : 4.740 \pm 2.232$	$\lambda_3 : 0.275 \pm 0.201$	$\lambda_7 : -0.002 \pm 0.463$	
	$\tilde{\alpha} : (0.4 \pm 38.3) \times 10^{-3}$	$\varsigma_u : -0.001 \pm 0.043$	$\varsigma_d : -0.005 \pm 0.613$	$\varsigma_l : -0.560 \pm 41.890$

Table 2. IC value and marginalised individual results. The mass limits are in GeV, at 95% probability, while for the other parameters we show the mean value and the standard deviation.

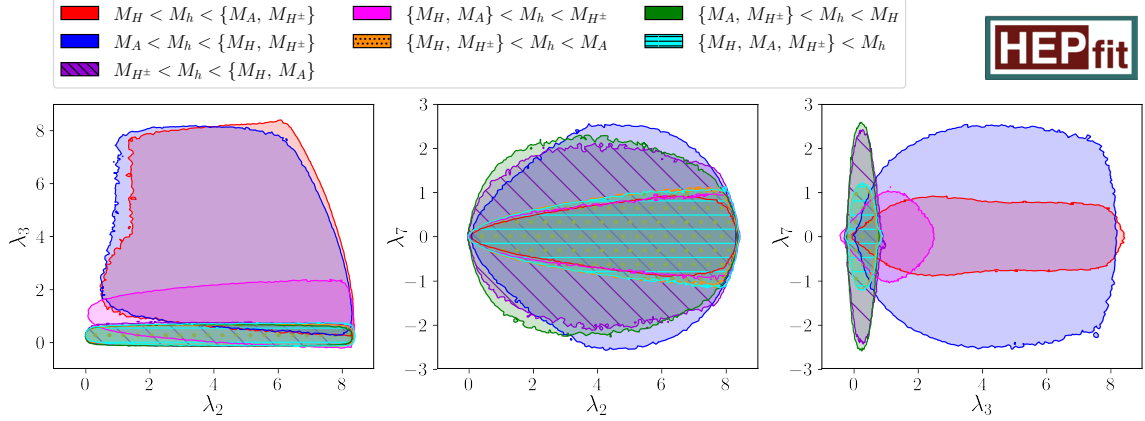


Figure 1. Correlations among the parameters of the scalar potential, shown as allowed regions with 95% probability.

the tree-level ones, as described in Sec. 3.2, provides, then, strong constraints on λ_3 and λ_7 . These constraints become stronger when $M_{H^\pm} \ll M_{\varphi_i^0}$, since the loop correction to $\lambda_{\varphi_i^0 H^+ H^-}$ scales as $1/M_{H^\pm}^2$, as can be seen in Eq. (3.9). When $M_{H^\pm} \gg M_{\varphi_i^0}$, the loop correction scales as $1/M_{\varphi_i^0}^2$, and we also get a strong constraint on the coupling of that neutral scalar with the charged scalar.² This explains the behaviour of the correlations in Fig. 1, where we see tight constraints on λ_7 when M_H is small, while wider ranges are allowed in those scenarios with a heavier M_H (blue, green, and purple regions). On the other hand, the constraints on λ_3 are looser when the charged scalar can be heavy (red, blue, and magenta regions). Note that in the magenta region, although we allow M_{H^\pm} to be heavy, the oblique parameters force the charged scalar to also be light because the other two scalars are both light.

Scalar masses.- Fig. 2 shows the correlations among the scalar masses, and the correlations among their mass splitting. There is a clear complementarity between the different scenarios considered, which is particularly noticeable in the correlation among the two neutral scalars. In order to satisfy the constraints from the oblique parameters, the mass of the charged scalar must align with one of the neutral scalar masses, hence the complementarity. When the two neutral scalars are forced to be light (magenta), M_{H^\pm} is also pushed to be small, even though we allow it to be heavy, as mentioned before. If we impose one of the neutral scalars to be light and the other to be heavy together with the charged scalar (blue/red), the splitting between the two heavy masses becomes small. When only the charged scalar is imposed to be light (purple), one of the two neutral scalars must also be light to align with the charged one. However, when the charged scalar is imposed to be light together with a neutral scalar (orange/green), the mass of the other neutral scalar can reach large values, as in those cases the oblique constraints are avoided with the alignment

²The perturbative constraint is also relevant in this limit, since the effective coupling $(\lambda_{\varphi_i^0 H^+ H^-})_{\text{eff}}$ determines the charged-scalar contribution to $\varphi_i^0 \rightarrow \gamma\gamma$.

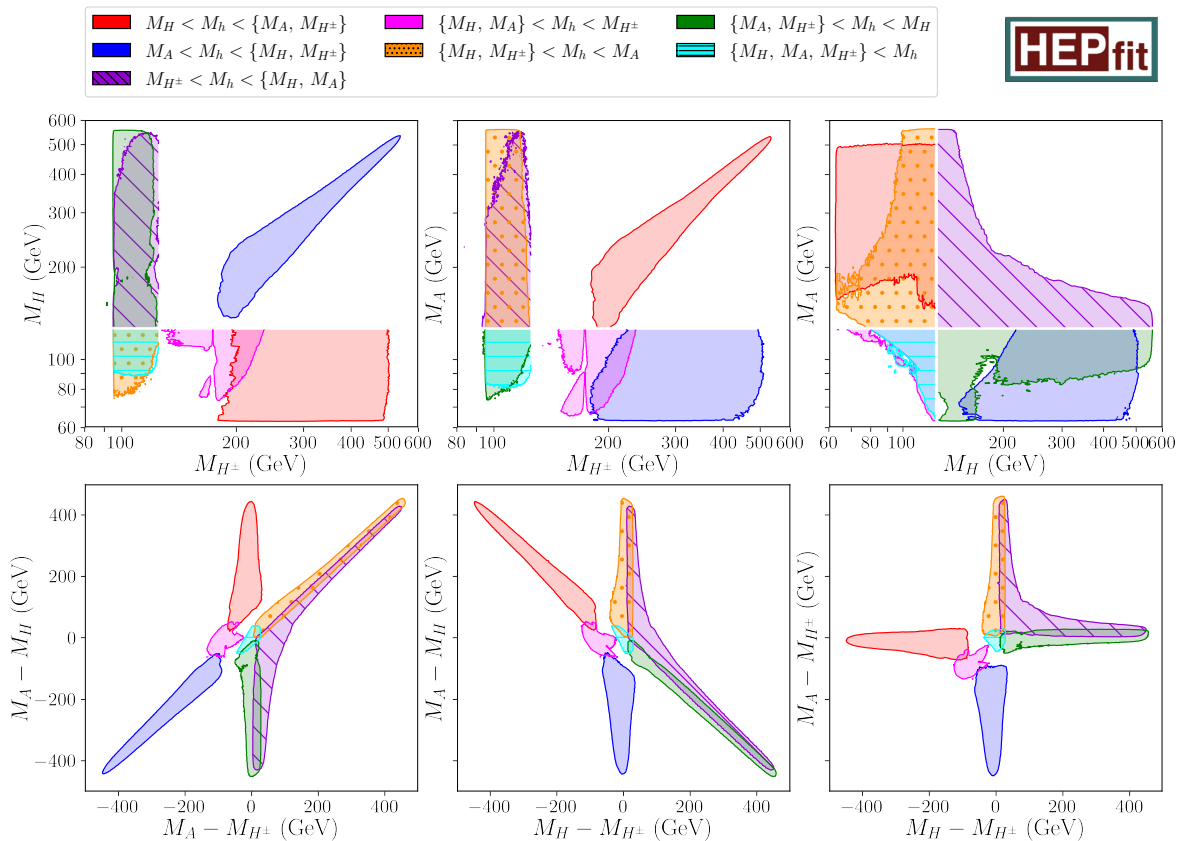


Figure 2. Correlations among the scalar masses and their mass splitting, shown as 95% allowed probability regions.

of the masses of the two light scalars.

In the scenario with three light scalars (cyan), the splitting of their masses is necessarily small, and for this reason the allowed region is found to be confined to the centre of all correlation plots among the scalar mass differences. Similarly, the scenario with two light neutral scalars (magenta) is also found to be in the central region of the same plots. Concerning the other scenarios, the alignment of the allowed regions along the mass-splitting axes can easily be understood from the corresponding ranges of allowed masses.

The theoretical constraints limit the maximum mass difference among all the scalars, disfavoring masses above 600 GeV when any scalar is lighter than the Higgs boson. The direct searches also play their role in imposing tight bounds on the masses, forcing the charged scalar to always be heavier than 90 GeV and the neutral scalars to be heavier than 60 GeV. These features are clearly seen in the correlation among the masses and the Yukawa alignment parameters, shown in Fig. 3.

Masses versus mixing angle and Yukawa alignment parameters.- As illustrated in Fig. 3, the constraint that neutral masses are to be heavier than 60 GeV cannot be avoided, even for small values of the other parameters. This limit arises because masses

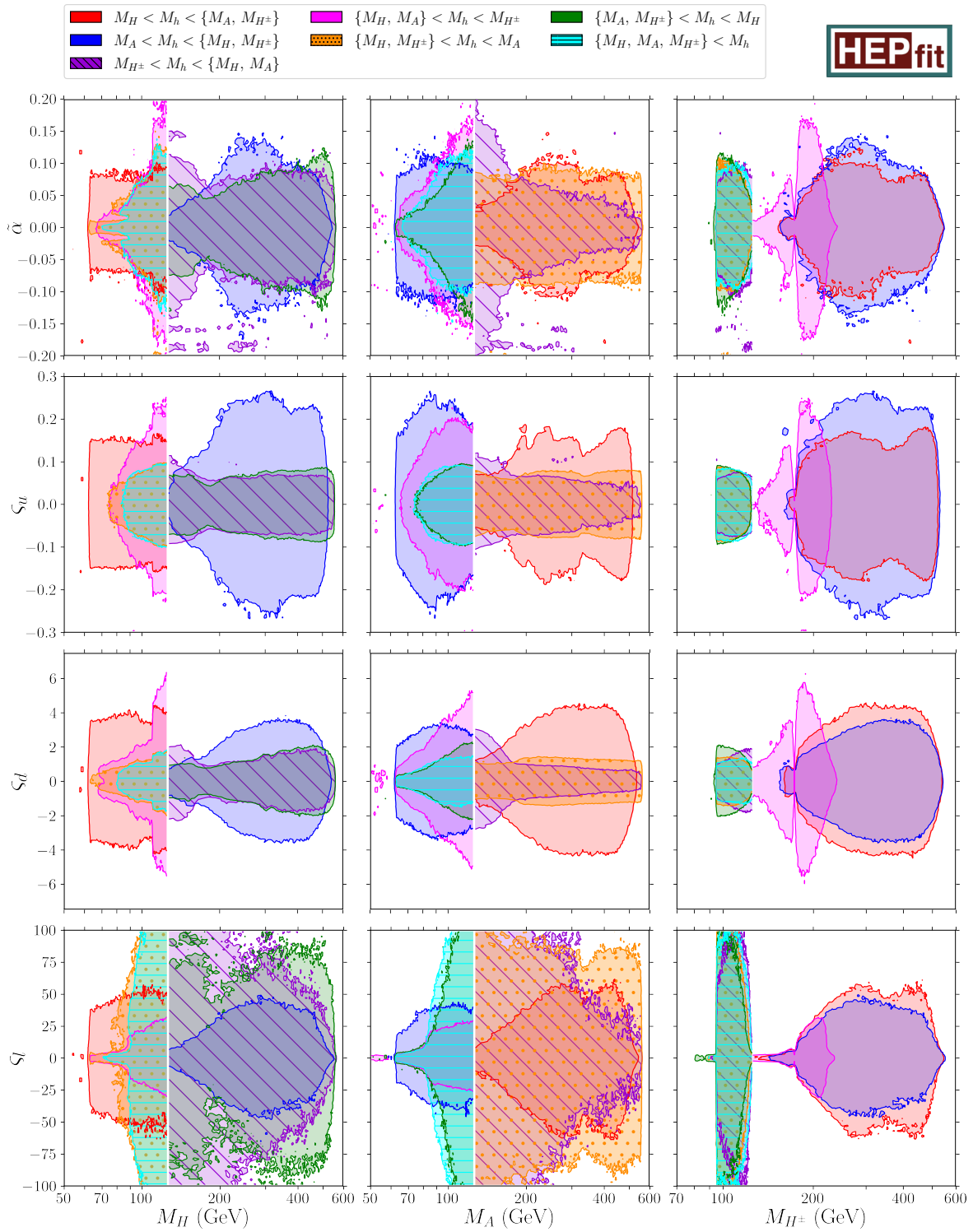


Figure 3. Correlations between the mixing angle (in rad) and the Yukawa alignment parameters with the scalar masses, shown as 95% allowed probability regions.

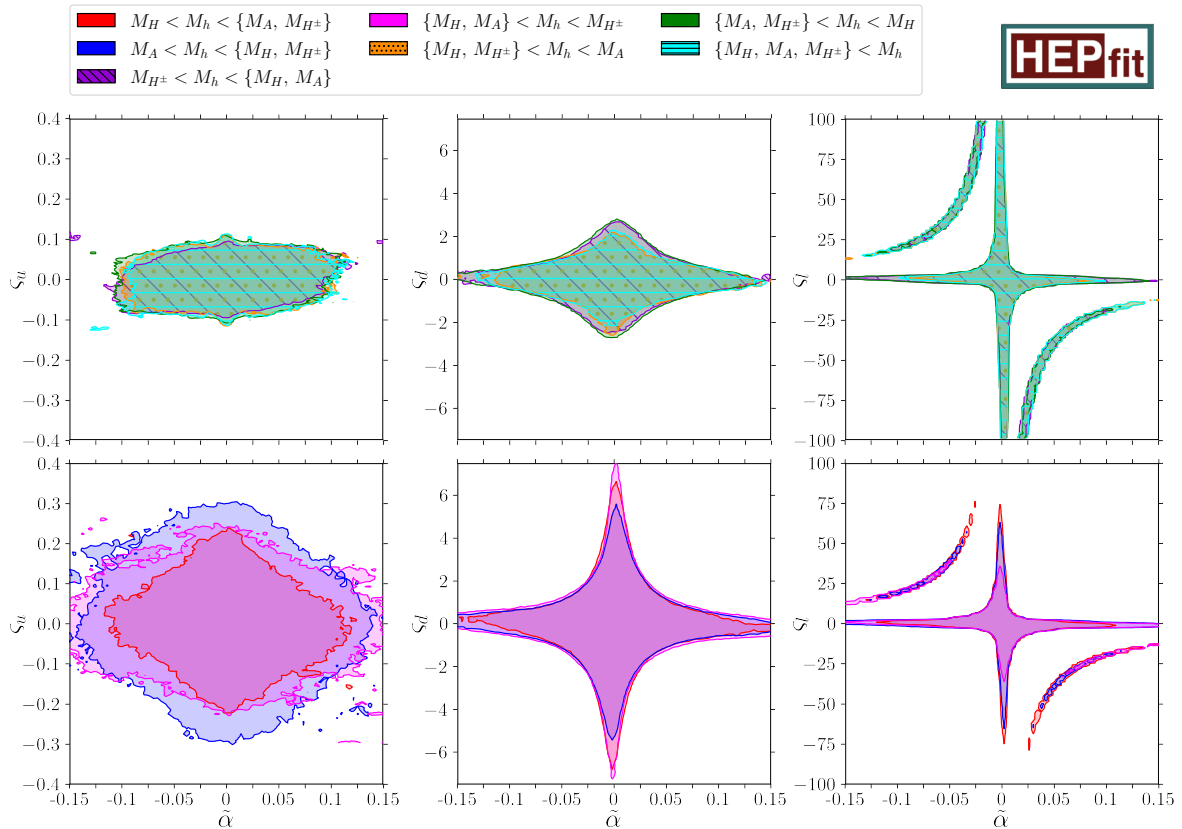


Figure 4. Correlations among the mixing angle (in rad) and the Yukawa alignment parameters, shown as 95% allowed probability regions. The panels are duplicated to facilitate readability. In the top panel we present the scenarios with M_{H^\pm} light, the rest are presented in the bottom panel.

below 60 GeV would enable the 125 GeV Higgs to decay into neutral scalars, a decay channel that has been extensively scrutinised by LHC experiments. By the same token, charged scalars lighter than 95 GeV are tightly constrained by the LEP searches for double production of charged scalars decaying to taus and quarks. Remarkably, for masses between 95 GeV and around 120 GeV the constraints on the leptonic coupling from direct searches exhibit a gap, which manifests as an allowed region including extremely high values for ζ_l . This region might have been scrutinised by the slepton searches that we have added in this analysis but, unfortunately, the slepton limits start above 120 GeV, and this is precisely why below that value we see the wider allowed region. In principle, flavour observables could also constrain this region, but the current limits on ζ_l are very weak. In those scenarios with a light charged scalar, flavour provides strong constraints on ζ_u and ζ_d , pushing these parameters to be small; this reduces significantly the sensitivity to the leptonic alignment parameter, so that values of ζ_l as high as 100 become allowed.

The dominant BSM contributions to flavour observables are mostly proportional to $\zeta_u^2 m_t^2 / M_{H^\pm}^2$, $\zeta_d^2 m_b^2 / M_{H^\pm}^2$, and $\zeta_u \zeta_d m_t m_b / M_{H^\pm}^2$, which enforces tight constraints on ζ_u and

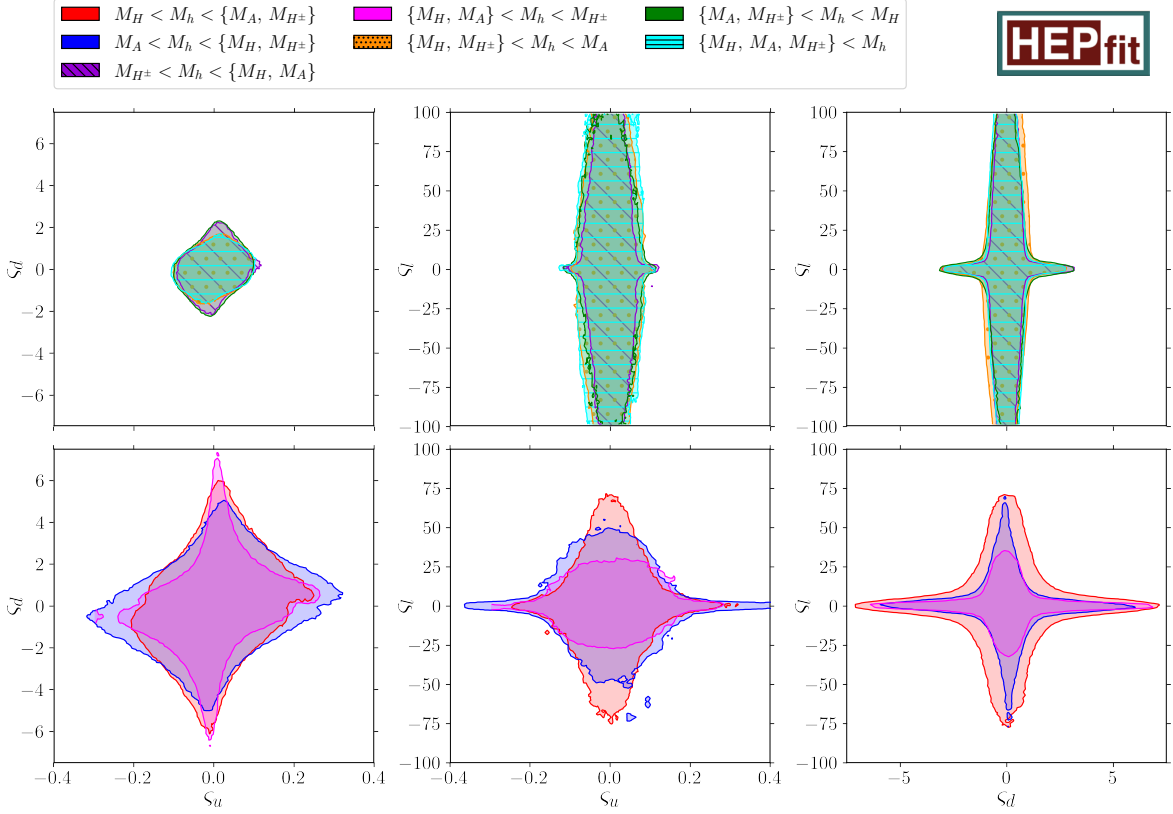


Figure 5. Correlations among the Yukawa alignment parameters, shown as 95% allowed probability regions. To facilitate readability, the results are provided with the same split in M_{H^\pm} scenarios as in Fig. 4.

somewhat softer upper bounds on ς_d . The allowed ranges for these two parameters get obviously broader at larger values of M_{H^\pm} (red, blue, and magenta regions). On the other hand, the LHC direct-detection observables restrict the combinations $\varsigma_u \varsigma_l$ and $\varsigma_d \varsigma_l$, where the $\varsigma_{u,d}$ parts come from the production channels involving quark-scalar vertices, and the ς_l part arises from the leptonic decay of the scalars. Therefore, the scenarios with larger masses of the charged scalar indirectly restrict ς_l to smaller ranges (red, blue, and magenta regions), whereas the scenarios with lighter M_{H^\pm} allow for comparatively larger values of ς_l (purple, orange, green, and cyan regions).

Owing to the good agreement of the Higgs signal-strengths with the SM expectations, the mixing $\tilde{\alpha}$ between the two \mathcal{CP} -even neutral scalars is bounded to be small in all scenarios, a visual confirmation, at the 95% probability region, of what we have already reported at the start of this section concerning the 68% probability ranges we obtained for this parameter.

Mixing angle versus Yukawa alignment parameters.- As shown in Fig. 4, the mixing angle is significantly correlated with the Yukawa alignment parameters. While the

measured Higgs coupling to the gauge bosons puts an absolute lower bound on $\cos \tilde{\alpha}$, the Yukawa couplings in Eq. (2.13) are sensitive to $\varsigma_f \sin \tilde{\alpha}$, providing a stronger constraint on $\tilde{\alpha}$ unless the alignment parameters are very small. Once these parameters are set to small values, the Higgs Yukawa couplings become extremely close to the SM prediction, for the values of the mixing angle considered here. The correlation with the up-type alignment parameter, shown in the left panels of Fig. 4, is broad, since the flavour observables already impose strong constraints on ς_u , suppressing its contribution to the signal strengths. The correlations are more visible in the centre (ς_d) and right (ς_l) panels. The leptonic alignment parameter exhibits two additional solutions where the measured absolute value of the Yukawa coupling is reached through a destructive interference between the $\cos \tilde{\alpha}$ and $\varsigma_l \sin \tilde{\alpha}$ contributions. This flipped-sign solution is not viable for the quark Yukawas, which are subject to strong constraints from other observables (like flavour and direct searches). As already pointed out, the scenarios with heavier H^\pm (red, blue, and magenta) are found to have larger allowed ranges of $\varsigma_{u,d}$ and smaller ones of ς_l .

Yukawa alignment parameters.- The correlations of the Yukawa alignment parameters among themselves are shown in Fig. 5. We can clearly see that, in the scenarios with a light charged scalar, both ς_u and ς_d are forced to be small, while much looser constraints are found for ς_l . As rationalised before, with such small values of the quark alignment parameters the flavour constraints become less sensitive to the lepton coupling. The correlations of the leptonic coupling with the quark ones clearly indicate that: in order to obtain values of ς_l as big as 100, the model needs to have very small values of $\varsigma_u \lesssim 0.1$ and $\varsigma_d \lesssim 1$; and in the scenarios where the quark couplings are allowed a bit more of free rein, ς_l compensates by getting increasingly squished in those regions of parameter space.

5.2 Effect of slepton searches

As already mentioned in Sec. 3.7, (left-handed) slepton searches at colliders with small neutralino masses can be reinterpreted as the search for a charged scalar decaying to a lepton and a neutrino because the two processes exhibit the same dilepton plus missing-energy signature in the final state. Although in our global fits we have incorporated the LEP and LHC slepton searches, in this subsection we address the influence they have on our results. There is a striking phenomenological difference between slepton and charged Higgs searches at colliders: the slepton decay usually conserves the lepton flavour, with a maximum of 5%–10% branching fraction permitted to lepton-flavour-violating decays [169] — as such, the experimental searches for sleptons assume lepton flavour conservation, i.e., a 100% probability to decay into a particular lepton. Yet, apart from a small branching fraction to $c\bar{b}$, a light charged Higgs has two dominant decay modes: $\tau^+\nu$ and $c\bar{s}$; if enough phase space is available, it can also decay significantly to $t\bar{b}$, and even $W^{+*}A$. After taking these branching fractions into account, the total cross section for the production of a pair of charged scalars and their subsequent decay into two specific leptons with missing energy may become substantially smaller than the one for the analogous slepton signature. Since the coupling of a charged Higgs to a charged lepton and a neutrino is proportional to the mass of the charged lepton in play, its electronic and muonic branching

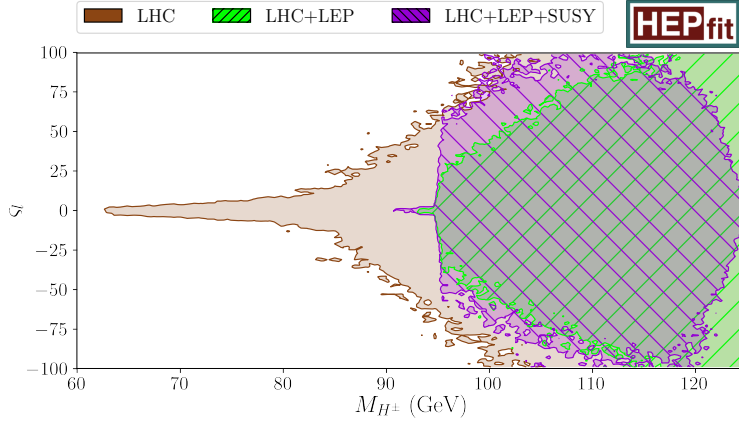


Figure 6. Correlation among ς_l and M_{H^\pm} after successive applications of direct search constraints. The region with all collider data included (purple) matches that from the global fit, shown in a different aspect ratio in Fig. 3.

fractions are negligible and, thus, the selectron and smuon searches from LEP and ATLAS (referenced in Tab. 17) put quite weak bounds on the parameters involved in charged Higgs phenomenology. The LEP bounds from stau searches are also weaker than the constraints arising from the direct LEP searches for a charged Higgs decaying to $\tau^+\nu$. Only the LHC stau searches have some non-negligible effect on the charged scalar parameters. However, the more stringent constraint on a light charged Higgs comes from the CMS $\tilde{\tau}_L$ search, which only applies for charged scalar masses heavier than 115 GeV [170].

Fig. 6 compares the constraints on the $\varsigma_l - M_{H^\pm}$ correlation emerging from direct searches at the LHC (all other constraints apart from the direct searches are also included) with those obtained after adding successively the LEP scalar searches and the SUSY searches. As can be seen, a global fit with direct searches from the LHC only (brown region) restricts the lower bound on the charged Higgs mass to 62.5 GeV (i.e. $M_h/2$), whereas the fit with direct search data from the LEP and the LHC (green region) pushes the lower bound on M_{H^\pm} to ~ 95 GeV. The slepton searches (purple) remove regions with higher values of $|\varsigma_l|$ for $115 \text{ GeV} < M_{H^\pm} < M_h$. As a result of constraining the masses above 115 GeV, the minimum of the likelihood shifts toward smaller M_{H^\pm} , where limits sensitive to $|\varsigma_l|$ from direct searches are absent. A consequence of this shift is that, at 95% probability, slightly higher values of $|\varsigma_l|$ become allowed when including the SUSY searches. Nevertheless, this effect diminishes on the regions with higher probability.

Because of the CMS $\tilde{\tau}_L$ search, the marginalised upper bound at 95% probability on a light charged Higgs mass does not reach M_h in some cases, as can be noticed from the last three scenarios in Tab. 2.

6 Implications of $(g - 2)_\mu$

Besides the set of flavour observables that was used to produce the results presented in the previous section, HEPfit contains a full implementation of the NP contribution to the anomalous magnetic moment of the muon, $a_\mu = (g - 2)_\mu/2$, based on Ref. [171], including

all relevant 1- and 2-loop contributions for the A2HDM [96, 172–179]. Unfortunately, the SM prediction of a_μ remains very uncertain due to a significant discrepancy between the estimated hadronic vacuum polarisation contribution derived from data-driven approaches, using dispersive e^+e^- data [180], and those obtained from τ -decay data [181, 182] or lattice QCD calculations, which can be seen in collected form in the publication with the latest computation from the BMW group [183]. The recent CMD-3 high-precision measurement of the $e^+e^- \rightarrow \pi^+\pi^-$ cross section [184, 185] shows in fact a very good compatibility with τ and lattice data, implying a much better agreement with the muon $g - 2$ measurement than previously estimated from e^+e^- data. Nevertheless, given all these discrepancies and the lack of consensus within the community, we have chosen not to include this observable in the main fit. However, we have evaluated its impact separately. In order to illustrate the implications of the different theoretical predictions, we have performed two different global fits:

1. Keeping all theoretical estimates from the 2020 white paper unchanged [180], but updating the experimental value of $(g - 2)_\mu$ to the most recent world average [186, 187], such that the difference between both becomes

$$\Delta a_\mu^{\text{WP}} = a_\mu^{\text{exp}} - a_\mu^{\text{SM, WP}} = 249 (49) \times 10^{-11}. \quad (6.1)$$

This claimed 5σ “anomaly” has triggered a large number of NP explanations, some of them involving light scalars [80, 95, 97, 138, 171, 188–194].

2. Adopting the latest BMW computations of the hadronic vacuum polarisation [183] and light-by-light scattering [195] contributions,

$$\Delta a_\mu^{\text{BMW}} = a_\mu^{\text{exp}} - a_\mu^{\text{SM, BMW}} = 4 (42) \times 10^{-11}, \quad (6.2)$$

in excellent agreement with the experimental measurement.

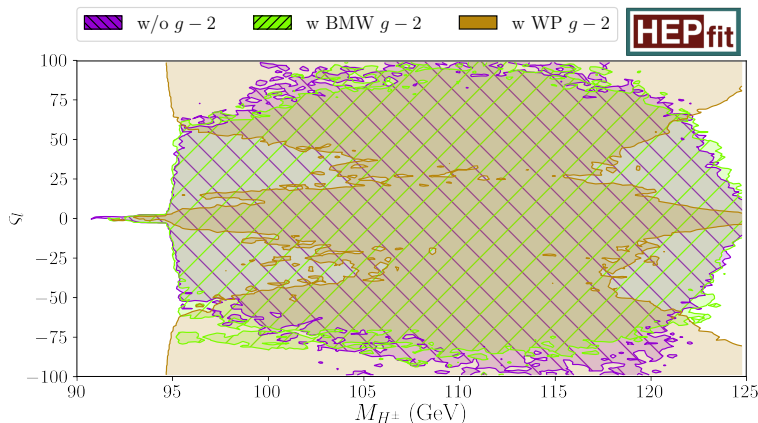


Figure 7. Allowed 95% probability regions for ς_l versus M_{H^\pm} for the global fit with the prior $M_{H^\pm} \leq M_h \leq M_{H,A}$, without including the observable $(g - 2)_\mu$ (purple, as in Fig. 3), adding the prediction of $(g - 2)_\mu$ from the 2020 white paper (brown), and adding the prediction of $(g - 2)_\mu$ from the BMW collaboration (green). The inputs used for the white paper and BMW scenarios can be found in Eqs. (6.1) and (6.2), respectively.

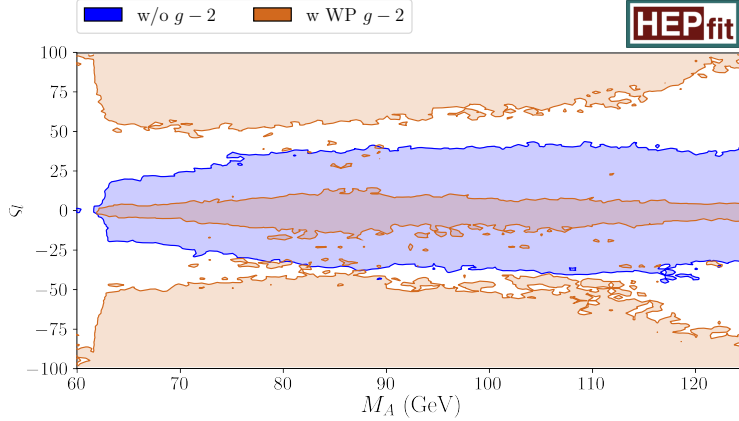


Figure 8. Allowed 95% probability regions for ς_l versus M_A for the global fit with the prior $M_A \leq M_h \leq M_{H,H^\pm}$, without including the observable $(g-2)_\mu$ (blue, as in Fig. 3) and adding the prediction of $(g-2)_\mu$ from the 2020 white paper (brown). The inputs used for the white paper scenario can be found in Eq. (6.1).

Following this initial exposition, we now assess how each Δa_μ above would affect our global analysis. 2HDM explanations of the so-called “ $g-2$ anomaly” require light scalar or pseudoscalar particles with large values of their leptonic couplings [171]. In order to maximise the possible effect, we focus on scenarios with $M_{H^\pm} < M_h$ because in this case there are insufficient observables to constrain ς_l below the perturbative limit of 100, at a 95% probability. Fig. 7 compares in the $M_{H^\pm} - \varsigma_l$ plane the allowed 95% probability region obtained without including $(g-2)_\mu$ (purple) with the ones emerging from global fits including $(g-2)_\mu$: either with the 2020 white paper (brown) or the latest BMW (green) SM predictions.

The impact of $(g-2)_\mu$ in the global fit is negligible when the SM theoretical prediction agrees with the experimental measurement because, with the current uncertainty, this observable is not able to further constrain ς_l . Since the BMW value is completely compatible with the experimental measurement, there is a perfect overlap between the purple and green regions in the figure.

The situation is very different if one employs the white paper prediction, which deviates from the experimental value by around 5 standard deviations. Reducing the tension with $(g-2)_\mu$ requires then larger values of ς_l . However, since all the other observables prefer smaller values of this parameter, a region with very small values of ς_l remains allowed at 95% probability. For this last region, the prediction for $(g-2)_\mu$ is obviously in huge tension, but the tension for all the other observables is reduced, while the opposite happens for the region with larger values of ς_l . This tension translates into a much worse performance of the fit. Indeed, the IC value for this fit is around 129, while for the fit with BMW data and for the fit without $(g-2)_\mu$, it is about 88. As evident from this difference of ~ 40 in ICs, which reflects the comparison of hypotheses as would be obtained with the calculation of the Bayes factor, the A2HDM model is clearly not a great solution to explain the tension between the $(g-2)_\mu$ predicted by the white paper and the experimental measurement.

The situation is similar for the other scenarios. Incorporating $(g-2)_\mu$ using the theoretical prediction of the white paper deteriorates significantly the quality of the fits. To provide another example, we compare, in Fig. 8, the corresponding fits for the case of a light pseudoscalar, a widely used model to explain the $(g-2)_\mu$ anomaly (see, e.g., the review presented in Ref. [138], and references therein). As found in the case of a light charged scalar, two clearly separated regions appear in this case, in such a way that performing an analysis with the input from the white paper generates also here a strong tension with the data. Therefore, a possible explanation of this anomaly with a light pseudoscalar within the A2HDM is, as is the case for any extra scalar from this model, extremely disfavoured once enough data are taken into account.

7 Conclusions

In this paper we have studied in great detail whether neutral and/or charged scalars lighter than the 125 GeV Higgs could be compatible with current data, within the framework of the A2HDM. The \mathcal{CP} -conserving A2HDM introduces ten independent BSM parameters: the masses of three new scalars (M_H, M_A , and M_{H^\pm}), three scalar-potential parameters (λ_2, λ_3 , and λ_7), three alignment parameters (ς_u, ς_d , and ς_l), and the angle $\tilde{\alpha}$ mixing the two \mathcal{CP} -even scalars. The following constraints have been imposed to restrict the parameter space of the model in the light-mass regime: vacuum stability, perturbativity, electroweak precision observables, flavour observables, Higgs signal strengths, and several relevant direct searches at high-energy colliders (LEP and LHC). We have performed our fits with the help of the open-source code `HEPfit`, which employs Bayesian statistics powered by a MCMC algorithm. Depending on the ranges attributed to the masses of the BSM scalars, seven different scenarios arise. According to the IC values obtained for each fit, all these seven scenarios show a similar adeptness at fitting the data, though the scenarios with only one light neutral scalar perform marginally better — in fact, the IC values of the latter are even identical to those from a fit with all scalars allowed to be heavy.

The measured (125 GeV) Higgs-boson properties at the LHC exclude that the neutral scalars could be lighter than half of the Higgs mass, at 95% probability. On the other hand, the LEP searches push the lower bound of the charged scalar mass to 95 GeV at the same probability. In all these light scenarios, the bounds from stability, perturbativity, and electroweak precision observables never allow the masses of the heavier scalars to reach beyond 560 GeV, at 95% probability. Interestingly, the same constraints restrict the mass of a heavy charged Higgs to be below 226 GeV when the two neutral scalars are taken to be light.

While the measurements of the Higgs signal strengths constrain the mixing angle $\tilde{\alpha}$ to a very small value, the stability and perturbativity bounds force λ_2 and λ_3 to be in the range $[0, 9]$, and λ_7 to be in the range $[-2.5, 2.5]$. The mass of the charged Higgs plays an important role in constraining the parameter λ_3 , whereas the mass of the new \mathcal{CP} -even scalar dictates the restriction on λ_7 through the effective cubic coupling $\lambda_{HH^+H^-}$ at one loop. Imposition of perturbativity at NLO level might restrict the scalar potential

couplings in a more stringent fashion. Such an improvement of the code dedicated to the A2HDM in `HEPfit` is currently being developed, and will be left for future analyses.

The alignment parameters are restricted by the constraints from Higgs signal strengths, flavour observables, and direct searches. Their correlations with the scalar mixing angle are governed by the Higgs signal strengths, while flavour observables control the correlations between the alignment parameters and the charged scalar mass. Since the dominant NP contributions to flavour observables are proportional to quadratic powers of $(\varsigma_{u,d}/M_{H^\pm})$, the scenarios with a heavier charged scalar permit larger values of $\varsigma_{u,d}$. On the other hand, the direct searches from the LHC provide restrictions to the combinations $\varsigma_{u\zeta_l}$ and $\varsigma_{d\zeta_l}$. Thus, larger values of M_{H^\pm} indirectly restrict ζ_l to lower values. Conversely, the scenarios with lighter H^\pm require smaller values of $\varsigma_{u,d}$, in order to obey the flavour constraints, and that, in turn, weakens the direct search limits on ζ_l , as patent in the wider allowed ranges shown by this model parameter.

As discussed in Secs. 3.7 and 5.2, the modes used by the LEP and LHC collaborations to look for the existence of sleptons exhibit a similar collider signature as those from probes of charged scalars decaying to $\tau^+\nu$, meaning that these searches can be taken into account while studying the phenomenology of the charged Higgs. It is, once more, worth of note that one should only consider the data from left-handed sleptons, as they share the same weak isospin with the charged Higgs. Moreover, while sleptons exhibit a dominant decay to a particular lepton flavour, the branching fractions of other H^\pm decay channels must be properly incorporated. With these considerations, we found that, among all the slepton searches, only the $\tilde{\tau}_L$ searches at the LHC have some influence on the A2HDM global fits. This effect is, however, not very drastic: it imposes restrictions on the parameter space allowed to ζ_l only for light charged scalar masses in the range of 115 GeV to 125 GeV.

Since the controversy about the SM prediction of $(g-2)_\mu$ has not been completely settled yet, we have not included this observable in our main global fits. Rather, we have presented, for the most favourable scenario with just a light charged scalar, the implications of two different theoretical estimates: that of the 2020 white paper, and the one derived from the latest BMW computations. As expected, the inclusion of the BMW results does not have any visible impact on the parameter space, as the lattice prediction of a_μ is now in perfect agreement with the experimental world average, whereas the result from the white paper tries to modify the ζ_l vs M_{H^\pm} correlation in such a way that the tension with the experimental value could be reduced with BSM scalar contributions. However, in terms of fit goodness, the inclusion of this $a_\mu^{\text{SM, WP}}$ from 2020 makes the resulting fit considerably worse. Future consensus on the SM predictions, if they go in the direction of the BMW computations, would put to rest this necessity for the A2HDM to solve a “ $g-2$ anomaly”. Even an updated white paper value, depending on how such an endeavour would combine current estimations to produce the theoretical state-of-the-art, should already reduce the tension from the 5σ level it presently sits at.

To summarise, although the current constraints on light scalars are quite strong, our fits demonstrate that ample regions of the A2HDM parameter space are still allowed in the seven possible scenarios. This should motivate a renewed experimental effort in the search for light scalar or pseudoscalar bosons.

Acknowledgements

We would like to acknowledge Milada M. Mühlleitner, Ulrich Nierste, Ayan Paul, Pablo Roig, Michael Spira, and Dominik Stöckinger, for useful comments which helped improve some of the fits here presented. A.P. would like to thank the high-energy physics group of the University of Granada for their hospitality during the time this article was being prepared. This work has been supported by MCIN/AEI/10.13039/501100011033 (grants PID2020-114473GB-I00, PID2023-146220NB-I00, and CEX2023-001292-S), by Generalitat Valenciana (grant PROMETEO/2021/071), by the European Research Council under the European Union’s Horizon 2020 research and innovation programme (grant agreement no. 949451), and by a Royal Society University Research Fellowship (grant no. URF/R1/201553).

Data availability statement

This manuscript has no associated data or the data will not be deposited. All the results in this paper can be reproduced using `HEPfit` (at commit [24ac2b1](#)) — following the procedures detailed in Ref. [101] — together with configuration files containing the prior ranges given in Tab. 1, examples of which may be provided upon request.

A Direct searches included

Here we provide the experimental direct searches that have been included in our analysis.

A.1 Collider searches for light neutral scalars

	Process	Range (GeV)	\sqrt{s} (TeV)	Ref.	
CMS Searches	$pp \rightarrow A(b\bar{b}) \rightarrow \tau^+\tau^-(b\bar{b})$	$25 < M_A < 80$	8	[196]	
	$pp \rightarrow h \rightarrow AA \rightarrow \tau^+\tau^-\tau^+\tau^-$	$5 < M_A < 15$		[197]	
	$pp \rightarrow h \rightarrow AA \rightarrow \mu^+\mu^-b\bar{b}$	$25 < M_A < 62.5$			
	$pp \rightarrow h \rightarrow AA \rightarrow \mu^+\mu^-\tau^+\tau^-$	$15 < M_A < 62.5$			
	$pp \rightarrow A(b\bar{b}) \rightarrow \mu^+\mu^-(b\bar{b})$	$25 < M_A < 60$			[198]
	$pp \rightarrow H \rightarrow \gamma\gamma$	$80 < M_H < 110$			[88]
	$pp \rightarrow h \rightarrow AA \rightarrow \mu^+\mu^-\tau^+\tau^-$	$15 < M_A < 62.5$	13	[199]	
	$pp \rightarrow h \rightarrow AA \rightarrow \tau^+\tau^-b\bar{b}$	$12 < M_A < 60$		[200]	
	$pp \rightarrow h \rightarrow AA \rightarrow \mu^+\mu^-b\bar{b}$	$15 < M_A < 62$		[200]	
	$pp \rightarrow A(b\bar{b}) \rightarrow \tau^+\tau^-(b\bar{b})$	$25 < M_A < 70$		[201]	
	$pp \rightarrow h \rightarrow AA \rightarrow \tau^+\tau^-\tau^+\tau^-$	$4 < M_A < 15$		[202]	
	$pp \rightarrow h \rightarrow \varphi_i^0(Z) \rightarrow \ell^+\ell^-(\ell^+\ell^-)$	$4 < M_{\varphi_i^0} < 60$		[203]	
	$pp \rightarrow h \rightarrow \varphi_i^0\varphi_i^0 \rightarrow \ell^+\ell^-\ell^+\ell^-$				
	$pp \rightarrow h \rightarrow AZ \rightarrow \gamma\gamma\ell^+\ell^-$	$1 < M_A < 30$		[204]	
	$pp \rightarrow h \rightarrow AA \rightarrow \gamma\gamma\gamma\gamma$	$15 < M_A < 62$		[205]	
	$pp \rightarrow h \rightarrow AA \rightarrow b\bar{b}b\bar{b}$	$15 < M_A < 60$		[206]	
	$pp \rightarrow \varphi_i^0(V) \rightarrow l^+l^-(l\nu/l^+l^-)$	$15 < M_{\varphi_i^0} < 350$		[207]	
	$pp \rightarrow \varphi_i^0(t\bar{t}) \rightarrow l^+l^-(t\bar{t})$				
	$pp \rightarrow H \rightarrow \gamma\gamma$	$70 < M_H < 110$		[89]	

Table 3. Relevant CMS searches for a light neutral scalar.

ATLAS Searches	Process	Range (GeV)	\sqrt{s} (TeV)	Ref.
	$pp \rightarrow h \rightarrow AA \rightarrow \tau^+ \tau^- \tau^+ \tau^-$	$3.7 < M_A < 50$	8	[208]
	$pp \rightarrow h \rightarrow AA \rightarrow \gamma\gamma\gamma\gamma$	$10 < M_A < 62$		[209]
	$pp \rightarrow h \rightarrow \varphi_i^0 \varphi_i^0 \rightarrow \gamma\gamma gg$	$20 < M_{\varphi_i^0} < 60$	13	[210]
	$pp \rightarrow h(V) \rightarrow \varphi_i^0 \varphi_i^0 (\ell^+ \ell^-) \rightarrow b\bar{b} b\bar{b} (\ell^+ \ell^-)$	$20 < M_{\varphi_i^0} < 60$		[211]
	$pp \rightarrow h \rightarrow \varphi_i^0 \varphi_i^0 \rightarrow \mu^+ \mu^- b\bar{b}$	$20 < M_{\varphi_i^0} < 60$		[212]
	$pp \rightarrow h(Z) \rightarrow \varphi_i^0 \varphi_i^0 (\ell^+ \ell^-) \rightarrow b\bar{b} b\bar{b} (\ell^+ \ell^-)$	$15 < M_{\varphi_i^0} < 30$		[213]
	$pp \rightarrow h \rightarrow AA \rightarrow \mu^+ \mu^- b\bar{b}$	$16 < M_A < 62$		[214]
	$pp \rightarrow h \rightarrow \varphi_i^0(Z) \rightarrow \mu^+ \mu^- (\ell^+ \ell^-)$	$15 < M_{\varphi_i^0} < 30$		[215]
	$pp \rightarrow h \rightarrow \varphi_i^0 \varphi_i^0 \rightarrow \mu^+ \mu^- \mu^+ \mu^-$	$1 < M_{\varphi_i^0} < 60$		
	$pp \rightarrow A(t\bar{t}) \rightarrow \mu^+ \mu^- (t\bar{t})$	$15 < M_A < 72$		[216]
	$pp \rightarrow h \rightarrow AA \rightarrow b\bar{b} \tau^+ \tau^-$	$12 < M_A < 60$		[217]
	$pp \rightarrow h \rightarrow AA \rightarrow \gamma\gamma\gamma\gamma$	$10 < M_A < 62$		[218]
	$gg \rightarrow A \rightarrow \tau^+ \tau^-$	$20 < M_A < 90$		[219]
	$pp \rightarrow H \rightarrow \gamma\gamma$	$66 < M_H < 110$		[90]

Table 4. Relevant ATLAS searches for a light neutral scalar.

LEP Searches	Process	Range (GeV)	\sqrt{s} (TeV)	Ref.
	$e^+ e^- \rightarrow \varphi_i^{\text{even}} Z \rightarrow \gamma\gamma Z$	$20 < M_{\varphi_i^{\text{even}}} < 116$	0.088 – 0.209	[220]
	$e^+ e^- \rightarrow \varphi_i^{\text{even}} Z \rightarrow b\bar{b} Z$	$12 < M_{\varphi_i^{\text{even}}} < 116$		
	$e^+ e^- \rightarrow \varphi_i^{\text{even}} Z \rightarrow \tau^+ \tau^- Z$			
	$e^+ e^- \rightarrow \varphi_i^0 \varphi_j^0 \rightarrow b\bar{b} b\bar{b}$	$15 < M_{\varphi_i^0} < 145$ $10 < M_{\varphi_j^0} < 105$	0.091 to 0.209	[221]
$e^+ e^- \rightarrow \varphi_i^0 \varphi_j^0 \rightarrow \tau^+ \tau^- \tau^+ \tau^-$	$5 < M_{\varphi_i^0} < 150$ $5 < M_{\varphi_j^0} < 100$			

Table 5. Relevant LEP searches for a neutral scalar.

A.2 Collider searches for heavy neutral scalars

CMS Searches	Process	Range (TeV)	\sqrt{s} (TeV)	Ref.
	$pp \rightarrow \varphi_i^0 \rightarrow hh \rightarrow (bb)(bb)$	$0.27 < M_{\varphi_i^0} < 1.1$	8	[222]
	$pp \rightarrow \varphi_i^0 \rightarrow hh \rightarrow (bb)(\gamma\gamma)$	$0.26 < M_{\varphi_i^0} < 1.1$		[223]
	$gg \rightarrow \varphi_i^0 \rightarrow hh \rightarrow (bb)(\tau\tau)$	$0.26 < M_{\varphi_i^0} < 0.35$		[224]
	$pp \rightarrow \varphi_i^0 \rightarrow hh[\rightarrow (bb)(\tau\tau)]$	$0.35 < M_{\varphi_i^0} < 1$		[225]
	$gg \rightarrow \varphi_i^0 \rightarrow hZ \rightarrow (bb)(\ell\ell)$	$0.225 < M_{\varphi_i^0} < 0.6$		[226]
	$gg \rightarrow \varphi_i^0 \rightarrow hZ \rightarrow (\tau\tau)(\ell\ell)$	$0.22 < M_{\varphi_i^0} < 0.35$		[224]
	$pp \rightarrow \varphi_3^0 \rightarrow \varphi_2^0 Z \rightarrow (bb)(\ell\ell)$	$0.04 < M_{\varphi_i^0} < 1$		[227]
	$pp \rightarrow \varphi_3^0 \rightarrow \varphi_2^0 Z \rightarrow (\tau\tau)(\ell\ell)$	$0.05 < M_{\varphi_i^0} < 1$		[227]
	$pp \rightarrow \varphi_i^0 \rightarrow hh \rightarrow (bb)(bb)$	$0.26 < M_{\varphi_i^0} < 1.2$	13	[228]
		$1 < M_{\varphi_i^0} < 3$		[229]
	$pp \rightarrow \varphi_i^0 \rightarrow hh[\rightarrow (WW)(WW)/(WW)(\tau\tau)/(\tau\tau)(\tau\tau)]$	$0.25 < M_{\varphi_i^0} < 1$		[230]
	$pp \rightarrow \varphi_i^0 \rightarrow hh \rightarrow (bb)(\gamma\gamma)$	$0.26 < M_{\varphi_i^0} < 1$		[231]
	$pp \rightarrow \varphi_i^0 \rightarrow hh \rightarrow (bb)(\tau\tau)$	$0.25 < M_{\varphi_i^0} < 0.9$		[232]
	$pp \rightarrow \varphi_i^0 \rightarrow hh[\rightarrow (bb)(\tau\tau)]$	$0.9 < M_{\varphi_i^0} < 4$		[233]
	$pp \rightarrow \varphi_i^0 \rightarrow hh \rightarrow (bb)(VV \rightarrow \ell\nu\ell\nu)$	$0.26 < M_{\varphi_i^0} < 0.9$		[234]
	$pp \rightarrow \varphi_i^0 \rightarrow hh[\rightarrow (bb)(WW \rightarrow q\bar{q}\ell\nu)]$	$0.8 < M_{\varphi_i^0} < 3.5$		[235]
	$pp \rightarrow \varphi_i^0 \rightarrow hh \rightarrow (bb)[ZZ \rightarrow \ell\ell jj]$	$0.26 < M_{\varphi_i^0} < 1$		[236]
	$pp \rightarrow \varphi_i^0 \rightarrow hh \rightarrow (bb)[ZZ \rightarrow \ell\nu\nu]$	$0.26 < M_{\varphi_i^0} < 1$		[236]
	$pp \rightarrow \varphi_i^0 \rightarrow hh[\rightarrow (bb)(WW/\tau\tau \rightarrow (q\bar{q}/\ell\nu)\ell\nu)]$	$0.8 < M_{\varphi_i^0} < 4.5$		[237]
	$0.25 < M_{\varphi_i^0} < 0.9$	[238]		
$gg \rightarrow \varphi_i^0 \rightarrow (h \rightarrow b\bar{b})[Z \rightarrow \nu\bar{\nu}/\ell\bar{\ell}]$	$0.22 < M_{\varphi_i^0} < 0.8$	[239]		
	$0.8 < M_{\varphi_i^0} < 2$	[240]		
$gg \rightarrow \varphi_i^0 \rightarrow (h \rightarrow \tau\tau)(Z \rightarrow \ell\ell)$	$0.22 < M_{\varphi_i^0} < 0.4$	[241]		
$bb \rightarrow \varphi_i^0 \rightarrow (h \rightarrow b\bar{b})[Z \rightarrow \nu\bar{\nu}/\ell\bar{\ell}]$	$0.22 < M_{\varphi_i^0} < 0.8$	[239]		
	$0.8 < M_{\varphi_i^0} < 2$	[240]		

Table 6. Direct searches in CMS for neutral heavy scalars, $\varphi_i^0 = H, A$, with final states including the Higgs boson or other neutral scalars. φ_3 denotes the heaviest scalar, $V = W, Z$, $\ell = e, \mu$. The parenthesis show the final decay of the SM particles produced from the NP particles. The square brackets are used when the values of $\sigma \cdot \mathcal{B}$ are shown in terms of the primary decay (i.e. the NP particle decay) but a particular decay channel of the SM particles is used to obtain those values.

ATLAS Searches	Process	Range (TeV)	\sqrt{s} (TeV)	Ref.
	$gg \rightarrow \varphi_i^0 \rightarrow hh$	$0.26 < M_{\varphi_i^0} < 1$	8	[242]
	$gg \rightarrow \varphi_i^0 \rightarrow hZ \rightarrow (bb)Z$	$0.22 < M_{\varphi_i^0} < 1$		[243]
	$gg \rightarrow \varphi_i^0 \rightarrow hZ \rightarrow (\tau\tau)Z$	$0.05 < M_{\varphi_i^0} < 1$		[243]
	$pp \rightarrow \varphi_i^0 \rightarrow hh[\rightarrow (bb)(bb)]$	$0.251 < M_{\varphi_i^0} < 5$	13	[244]
	$pp \rightarrow \varphi_i^0 \rightarrow hh[\rightarrow (bb)(\gamma\gamma)]$	$0.251 < M_{\varphi_i^0} < 1$		[245]
	$pp \rightarrow \varphi_i^0 \rightarrow hh[\rightarrow (bb)(\tau\tau)]$	$0.251 < M_{\varphi_i^0} < 1.6$		[246]
		$1 < M_{\varphi_i^0} < 3$		[247]
	$pp \rightarrow \varphi_i^0 \rightarrow hh[\rightarrow (bb)(WW)]$	$0.5 < M_{\varphi_i^0} < 3$		[248]
	$gg \rightarrow \varphi_i^0 \rightarrow hh \rightarrow (\gamma\gamma)(WW)$	$0.26 < M_{\varphi_i^0} < 0.5$		[249]
	$gg \rightarrow \varphi_i^0 \rightarrow hZ[\rightarrow (bb)Z]$	$0.22 < M_{\varphi_i^0} < 2$		[250]
	$bb \rightarrow \varphi_i^0 \rightarrow hZ[\rightarrow (bb)Z]$			
	$gg \rightarrow \varphi_3^0 \rightarrow \varphi_2^0 Z \rightarrow (bb)Z$	$0.13 < M_{\varphi_3^0} < 0.7$		[251]
	$bb \rightarrow \varphi_3^0 \rightarrow \varphi_2^0 Z \rightarrow (bb)Z$	$0.23 < M_{\varphi_2^0} < 0.8$		
$gg \rightarrow \varphi_3^0 \rightarrow \varphi_2^0 Z \rightarrow (WW)Z$	$0.2 < M_{\varphi_3^0} < 0.7 / 0.3 < M_{\varphi_2^0} < 0.8$			

Table 7. Direct searches in ATLAS for neutral heavy scalars, $\varphi_i^0 = H, A$, with final states including the Higgs boson or other neutral scalars. φ_3 denotes the heaviest scalar, $V = W, Z$, $\ell = e, \mu$. The parenthesis show the final decay of the SM particles produced from the NP particles. The square brackets are used when the values of $\sigma \cdot \mathcal{B}$ are shown in terms of the primary decay (i.e. the NP particle decay) but a particular decay channel of the SM particles is used to obtain those values.

CMS Searches	Process	Range (TeV)	\sqrt{s} (TeV)	Ref.
	$pp \rightarrow \varphi_i^0 \rightarrow Z\gamma \rightarrow (\ell\ell)\gamma$	$0.2 < M_{\varphi_i^0} < 1.2$	8	[252]
	$pp \rightarrow \varphi_i^0 \rightarrow VV$	$0.145 < M_{\varphi_i^0} < 1$		[253]
	$gg \rightarrow \varphi_i^0 \rightarrow \gamma\gamma$	$0.6 < M_{\varphi_i^0} < 5$	13	[254]
	$pp \rightarrow \varphi_i^0 \rightarrow Z\gamma[\rightarrow (\ell\ell \& qq)\gamma]$	$0.35 < M_{\varphi_i^0} < 4$		[255]
	$pp \rightarrow \varphi_i^0 \rightarrow ZZ[\rightarrow (\ell\ell)(qq, \nu\nu, \ell\ell)]$	$0.13 < M_{\varphi_i^0} < 3$		[256]
	$pp \rightarrow \varphi_i^0 \rightarrow ZZ[\rightarrow (qq)(\nu\nu)]$	$1 < M_{\varphi_i^0} < 4$		[257]
	$VV \rightarrow \varphi_i^0 \rightarrow WW$	$0.2 < M_{\varphi_i^0} < 3$		[258]
	$gg \rightarrow \varphi_i^0 \rightarrow WW$			
	$pp \rightarrow \varphi_i^0 \rightarrow WW[\rightarrow (\ell\nu)(qq)]$	$1 < M_{\varphi_i^0} < 4.4$		[259]
	$gg \rightarrow \varphi_i^0 \rightarrow WW$	$1 < M_{\varphi_i^0} < 4.5$		[260]
	$VV \rightarrow \varphi_i^0 \rightarrow WW$			
	$(gg+VV) \rightarrow \varphi_i^0 \rightarrow WW \rightarrow (\ell\nu)(\ell\nu)$	$0.2 < M_{\varphi_i^0} < 1$		[261]

Table 8. Direct searches in CMS for neutral heavy scalars, $\varphi_i^0 = H, A$, with vector-boson final states. $V = W, Z$, $\ell = e, \mu$. The parenthesis show the final decay of the SM particles produced from the NP particles. The square brackets are used when the values of $\sigma \cdot \mathcal{B}$ are shown in terms of the primary decay (i.e. the NP particle decay) but a particular decay channel of the SM particles is used to obtain those values.

ATLAS Searches	Process	Range (TeV)	\sqrt{s} (TeV)	Ref.
	$gg \rightarrow \varphi_i^0 \rightarrow \gamma\gamma$	$0.065 < M_{\varphi_i^0} < 0.6$	8	[262]
	$pp \rightarrow \varphi_i^0 \rightarrow Z\gamma \rightarrow (\ell\ell)\gamma$	$0.2 < M_{\varphi_i^0} < 1.6$		[263]
	$gg \rightarrow \varphi_i^0 \rightarrow ZZ$	$0.14 < M_{\varphi_i^0} < 1$		[264]
	$gg \rightarrow \varphi_i^0 \rightarrow WW$	$0.3 < M_{\varphi_i^0} < 1.5$		[265]
	$VV \rightarrow \varphi_i^0 \rightarrow WW$			
	$pp \rightarrow \varphi_i^0 \rightarrow \gamma\gamma$	$0.15 < M_{\varphi_i^0} < 3$	13	[266]
	$gg \rightarrow \varphi_i^0 \rightarrow Z\gamma[\rightarrow (\ell\ell)\gamma]$	$0.22 < M_{\varphi_i^0} < 3.4$		[267]
	$gg \rightarrow \varphi_i^0 \rightarrow Z\gamma[\rightarrow (qq)\gamma]$	$1.02 < M_{\varphi_i^0} < 6.8$		[268]
	$gg \rightarrow \varphi_i^0 \rightarrow ZZ[\rightarrow (\ell\ell)(\ell\ell, \nu\nu)]$	$0.2 < M_{\varphi_i^0} < 2$		[269]
	$VV \rightarrow \varphi_i^0 \rightarrow ZZ[\rightarrow (\ell\ell)(\ell\ell, \nu\nu)]$			
	$gg \rightarrow \varphi_i^0 \rightarrow ZZ[\rightarrow (\ell\ell, \nu\nu)(qq)]$	$0.3 < M_{\varphi_i^0} < 3$		[270]
	$VV \rightarrow \varphi_i^0 \rightarrow ZZ[\rightarrow (\ell\ell, \nu\nu)(qq)]$			
	$gg \rightarrow \varphi_i^0 \rightarrow WW[\rightarrow (e\nu)(\mu\nu)]$	$0.2 < M_{\varphi_i^0} < 4$		[271]
	$VV \rightarrow \varphi_i^0 \rightarrow WW[\rightarrow (e\nu)(\mu\nu)]$			
	$gg \rightarrow \varphi_i^0 \rightarrow WW[\rightarrow (\ell\nu)(qq)]$	$0.3 < M_{\varphi_i^0} < 3$		[272]
	$VV \rightarrow \varphi_i^0 \rightarrow WW[\rightarrow (\ell\nu)(qq)]$			
	$pp \rightarrow \varphi_i^0 \rightarrow VV[\rightarrow (qq)(qq)]$	$1.2 < M_{\varphi_i^0} < 3$		[273]
	$gg \rightarrow \varphi_i^0 \rightarrow VV$	$0.2 < M_{\varphi_i^0} < 5.2$		[274]
	$VV \rightarrow \varphi_i^0 \rightarrow VV$			

Table 9. Direct searches in ATLAS for neutral heavy scalars, $\varphi_i^0 = H, A$, with vector-boson final states. $V = W, Z$, $\ell = e, \mu$. The parenthesis show the final decay of the SM particles produced from the NP particles. The square brackets are used when the values of $\sigma \cdot \mathcal{B}$ are shown in terms of the primary decay (i.e. the NP particle decay) but a particular decay channel of the SM particles is used to obtain those values.

CMS Searches	Process	Range (TeV)	\sqrt{s} (TeV)	Ref.
	$bb \rightarrow \varphi_i^0 \rightarrow bb$	$0.1 < M_{\varphi_i^0} < 0.9$	8	[275]
	$gg \rightarrow \varphi_i^0 \rightarrow bb$	$0.33 < M_{\varphi_i^0} < 1.2$		[276]
	$bb \rightarrow \varphi_i^0 \rightarrow \mu\mu$	$0.12 < M_{\varphi_i^0} < 0.5$		[277]
	$gg \rightarrow \varphi_i^0 \rightarrow \mu\mu$			
	$bb \rightarrow \varphi_i^0 \rightarrow \tau\tau$	$0.09 < M_{\varphi_i^0} < 1$		[278]
	$gg \rightarrow \varphi_i^0 \rightarrow \tau\tau$			
	$tt/tW/tq \rightarrow \varphi_i^0 \rightarrow tt$	$0.35 < M_{\varphi_i^0} < 0.65$	13	[279]
	$pp \rightarrow \varphi_i^0 \rightarrow bb$	$0.55 < M_{\varphi_i^0} < 1.2$		[280]
		$0.05 < M_{\varphi_i^0} < 0.35$		[281]
	$bb \rightarrow \varphi_i^0 \rightarrow bb$	$0.3 < M_{\varphi_i^0} < 1.3$		[282]
	$bb \rightarrow \varphi_i^0 \rightarrow \mu\mu$	$0.14 < M_{\varphi_i^0} < 1$		[283]
	$gg \rightarrow \varphi_i^0 \rightarrow \mu\mu$			
	$bb \rightarrow \varphi_i^0 \rightarrow \tau\tau$	$0.06 < M_{\varphi_i^0} < 3.5$		[284]
$gg \rightarrow \varphi_i^0 \rightarrow \tau\tau$				

Table 10. Direct searches in CMS for neutral heavy scalars, $\varphi_i^0 = H, A$, with quarks and leptons ($\ell = e, \mu$) final states.

ATLAS Searches	Process	Range (TeV)	\sqrt{s} (TeV)	Ref.
	$gg \rightarrow \varphi_i^0 \rightarrow \tau\tau$	$0.09 < M_{\varphi_i^0} < 1$	8	[285]
	$bb \rightarrow \varphi_i^0 \rightarrow \tau\tau$			
	$bb \rightarrow \varphi_i^0 \rightarrow tt$	$0.4 < M_{\varphi_i^0} < 1$	[286]	
	$tt \rightarrow \varphi_i^0 \rightarrow tt$		[287]	
	$pp \rightarrow \varphi_i^0 \rightarrow bb$ (≥ 1 b-jet)	$1.4 < M_{\varphi_i^0} < 6.6$	13	[288]
	$pp \rightarrow \varphi_i^0 \rightarrow bb$	$0.6 < M_{\varphi_i^0} < 1.25$		
		$1.25 < M_{\varphi_i^0} < 6.2$		
	$bb \rightarrow \varphi_i^0 \rightarrow bb$	$0.45 < M_{\varphi_i^0} < 1.4$		[289]
	$bb \rightarrow \varphi_i^0 \rightarrow \mu\mu$	$0.2 < M_{\varphi_i^0} < 1$		[290]
	$gg \rightarrow \varphi_i^0 \rightarrow \mu\mu$			
	$bb \rightarrow \varphi_i^0 \rightarrow \tau\tau$	$0.2 < M_{\varphi_i^0} < 2.5$		[291]
	$gg \rightarrow \varphi_i^0 \rightarrow \tau\tau$			

Table 11. Direct searches in ATLAS for neutral heavy scalars, $\varphi_i^0 = H, A$, with quarks and leptons ($\ell = e, \mu$) final states.

A.3 Collider searches for charged scalars

CMS Searches	Process	Range (GeV)	\sqrt{s} (TeV)	Ref.
	$t \rightarrow (H^+ \rightarrow \tau^+\nu) b$	$80 < M_{H^+} < 160$	8	[292]
	$t \rightarrow (H^+ \rightarrow c\bar{s} = 100\%) b$	$90 < M_{H^+} < 160$		[293]
	$t \rightarrow (H^+ \rightarrow c\bar{b} = 100\%) b$	$90 < M_{H^+} < 150$		[294]
	$t \rightarrow b(H^+ \rightarrow W^+A) \rightarrow b(W^+\mu^+\mu^-)$	$15 < M_A < 75$ $100 < M_{H^+} < 160$	13	[295]
	$t \rightarrow (H^+ \rightarrow c\bar{s} = 100\%) b$	$80 < M_{H^+} < 160$		[296]

Table 12. Relevant CMS searches for a light charged scalar.

ATLAS Searches	Process	Range (GeV)	\sqrt{s} (TeV)	Ref.
	$t \rightarrow (H^+ \rightarrow \tau^+\nu) b$	$80 < M_{H^+} < 160$	8	[297]
	$t \rightarrow (H^+ \rightarrow c\bar{b}) b$	$60 < M_{H^+} < 160$	13	[298]
	$t \rightarrow b(H^+ \rightarrow W^+A) \rightarrow b(W^+\mu^+\mu^-)$	$15 < M_A < 72$ $120 < M_{H^+} < 160$		[216]
	$t \rightarrow (H^+ \rightarrow c\bar{s}) b$	$60 < M_{H^+} < 168$		[299]

Table 13. Relevant ATLAS searches for a light charged scalar.

LEP Searches	Process	Range (GeV)	\sqrt{s} (TeV)	Ref.
	$e^+e^- \rightarrow H^+H^- \rightarrow \tau^+\nu\tau^-\bar{\nu}$	$43 < M_{H^+} < 95$	0.183 to 0.209	[300]
	$e^+e^- \rightarrow H^+H^- \rightarrow q\bar{q}q\bar{q}$			
	$e^+e^- \rightarrow H^+H^- \rightarrow q\bar{q}\tau^-\bar{\nu}$	$50 < M_{H^+} < 93$		[301]
	$e^+e^- \rightarrow H^+H^- \rightarrow (A \rightarrow b\bar{b})W^{+*}(A \rightarrow b\bar{b})W^{-*}$	$12 < M_A < M_{H^+}$		
$e^+e^- \rightarrow H^+H^- \rightarrow (A \rightarrow b\bar{b})W^{+*}\tau^-\bar{\nu}$	$40 < M_{H^+} < 94$			

Table 14. Relevant LEP searches for a light charged scalar.

	Process	Range (TeV)	\sqrt{s} (TeV)	Ref.
CMS	$pp \rightarrow H^\pm \rightarrow \tau^\pm \nu$	$0.18 < M_{H^\pm} < 0.6$	8	[292]
	$pp \rightarrow H^\pm \rightarrow tb$			
	$pp \rightarrow H^\pm \rightarrow \tau^\pm \nu$	$0.08 < M_{H^\pm} < 3$	13	[302]
	$pp \rightarrow H^\pm \rightarrow tb$	$0.2 < M_{H^\pm} < 3$		[303]
ATLAS	$pp \rightarrow H^\pm \rightarrow \tau^\pm \nu$	$0.18 < M_{H^\pm} < 1$	8	[297]
	$pp \rightarrow H^\pm \rightarrow tb$	$0.2 < M_{H^\pm} < 0.6$		[304]
	$pp \rightarrow H^\pm \rightarrow \tau^\pm \nu$	$0.09 < M_{H^\pm} < 2$	13	[305]
	$pp \rightarrow H^\pm \rightarrow tb$	$0.2 < M_{H^\pm} < 2$		[306]

Table 15. Relevant CMS and ATLAS searches for a heavy charged scalars.

A.4 Other measurements

Expt.	Observable	Value	\sqrt{s} (TeV)	Ref.
ATLAS	$\mathcal{B}(h \rightarrow \text{invisible})$	$< 10.7\%$	13	[307]
LEP	$\Gamma(Z \rightarrow \text{invisible})$	(0.499 ± 0.0015) GeV	$0.088 - 0.094$	[10]
CMS		(0.523 ± 0.016) GeV	13	[308]
LEP	$\Gamma(W \rightarrow \text{invisible})$	(0.032 ± 0.060) GeV	$0.161 - 0.183$	[309]
CMS	$\Gamma(\text{top})$	(1.36 ± 0.127) GeV	8	[310]

Table 16. Relevant branching fractions and decay widths of heavy SM particles [311].

Expt.	Process	Range (GeV)	\sqrt{s} (TeV)	Ref.
LEP	$\tilde{l}^+ \tilde{l}^- \rightarrow l^+ l^- + 2\tilde{\chi}^0$	$45 < M_{\tilde{l}} < 102$	$0.183 - 0.208$	[312]
ATLAS	$\tilde{\ell}^+ \tilde{\ell}^- \rightarrow \ell^+ \ell^- + 2\tilde{\chi}^0$	$90 < M_{\tilde{\ell}} < 350$	13	[313]
	$\tilde{\tau}_L^+ \tilde{\tau}_L^- \rightarrow \tau^+ \tau^- + 2\tilde{\chi}^0$	$80 < M_{\tilde{\tau}} < 450$		[314]
CMS	$\tilde{\ell}^+ \tilde{\ell}^- \rightarrow \ell^+ \ell^- + 2\tilde{\chi}^0$	$100 < M_{\tilde{\ell}} < 800$	13	[315]
	$\tilde{\tau}_L^+ \tilde{\tau}_L^- \rightarrow \tau^+ \tau^- + 2\tilde{\chi}^0$	$90 < M_{\tilde{\tau}} < 500$		[170]

Table 17. Slepton searches at the LEP and the LHC. Here, l stands for three flavours of charged leptons whereas ℓ indicates electron or muon. These searches can be reinterpreted as charged Higgs searches.

References

- [1] ATLAS collaboration, *Observation of a new particle in the search for the Standard Model Higgs boson with the ATLAS detector at the LHC*, *Phys. Lett. B* **716** (2012) 1 [[1207.7214](#)].
- [2] CMS collaboration, *Observation of a New Boson at a Mass of 125 GeV with the CMS Experiment at the LHC*, *Phys. Lett. B* **716** (2012) 30 [[1207.7235](#)].
- [3] R. Oerter, *The Theory of Almost Everything: The Standard Model, the Unsung Triumph of Modern Physics*, Plume, New York, USA (2006).
- [4] M. Gell-Mann, *The interpretation of the new particles as displaced charge multiplets*, *Nuovo Cim.* **4** (1956) 848.
- [5] T.H. White, *The Once and Future King*, Collins, London, UK (1958).
- [6] J.L. Diaz-Cruz and D.A. Lopez-Falcon, *Probing the mechanism of EWSB with a rho parameter defined in terms of Higgs couplings*, *Phys. Lett. B* **568** (2003) 245 [[hep-ph/0304212](#)].
- [7] ATLAS, CMS collaboration, *Measurements of the Higgs boson production and decay rates and constraints on its couplings from a combined ATLAS and CMS analysis of the LHC pp collision data at $\sqrt{s} = 7$ and 8 TeV*, *JHEP* **08** (2016) 045 [[1606.02266](#)].
- [8] V. Ilisie and A. Pich, *QCD exotics versus a Standard Model Higgs*, *Phys. Rev. D* **86** (2012) 033001 [[1202.3420](#)].
- [9] UTFIT collaboration, *New UTfit Analysis of the Unitarity Triangle in the Cabibbo-Kobayashi-Maskawa scheme*, *Rend. Lincei Sci. Fis. Nat.* **34** (2023) 37 [[2212.03894](#)].
- [10] ALEPH, DELPHI, L3, OPAL, SLD, LEP ELECTROWEAK WORKING GROUP, SLD ELECTROWEAK GROUP, SLD HEAVY FLAVOUR GROUP collaboration, *Precision electroweak measurements on the Z resonance*, *Phys. Rept.* **427** (2006) 257 [[hep-ex/0509008](#)].
- [11] G.C. Branco, P.M. Ferreira, L. Lavoura, M.N. Rebelo, M. Sher and J.P. Silva, *Theory and phenomenology of two-Higgs-doublet models*, *Phys. Rept.* **516** (2012) 1 [[1106.0034](#)].
- [12] J.F. Gunion, H.E. Haber, G.L. Kane and S. Dawson, *The Higgs Hunter's Guide*, vol. 80, CRC Press, Boca Raton, USA (2000), [10.1201/9780429496448](#).
- [13] T.D. Lee, *A Theory of Spontaneous T Violation*, *Phys. Rev. D* **8** (1973) 1226.
- [14] Y.L. Wu and L. Wolfenstein, *Sources of CP violation in the two Higgs doublet model*, *Phys. Rev. Lett.* **73** (1994) 1762 [[hep-ph/9409421](#)].
- [15] F.J. Botella and J.P. Silva, *Jarlskog - like invariants for theories with scalars and fermions*, *Phys. Rev. D* **51** (1995) 3870 [[hep-ph/9411288](#)].
- [16] J.F. Gunion and H.E. Haber, *Conditions for CP-violation in the general two-Higgs-doublet model*, *Phys. Rev. D* **72** (2005) 095002 [[hep-ph/0506227](#)].
- [17] B. Grzadkowski, O.M. Ogreid and P. Osland, *Diagnosing CP properties of the 2HDM*, *JHEP* **01** (2014) 105 [[1309.6229](#)].
- [18] V. Keus, S.F. King, S. Moretti and K. Yagyu, *CP Violating Two-Higgs-Doublet Model: Constraints and LHC Predictions*, *JHEP* **04** (2016) 048 [[1510.04028](#)].
- [19] C.-Y. Chen, H.-L. Li and M. Ramsey-Musolf, *CP-Violation in the Two Higgs Doublet Model: from the LHC to EDMs*, *Phys. Rev. D* **97** (2018) 015020 [[1708.00435](#)].
- [20] S. Iguro and Y. Omura, *The direct CP violation in a general two Higgs doublet model*, *JHEP* **08** (2019) 098 [[1905.11778](#)].

- [21] E. Ma, *Verifiable radiative seesaw mechanism of neutrino mass and dark matter*, *Phys. Rev. D* **73** (2006) 077301 [[hep-ph/0601225](#)].
- [22] M. Hirsch, R.A. Lineros, S. Morisi, J. Palacio, N. Rojas and J.W.F. Valle, *WIMP dark matter as radiative neutrino mass messenger*, *JHEP* **10** (2013) 149 [[1307.8134](#)].
- [23] R. Barbieri, L.J. Hall and V.S. Rychkov, *Improved naturalness with a heavy Higgs: An Alternative road to LHC physics*, *Phys. Rev. D* **74** (2006) 015007 [[hep-ph/0603188](#)].
- [24] L. Lopez Honorez, E. Nezri, J.F. Oliver and M.H.G. Tytgat, *The Inert Doublet Model: An Archetype for Dark Matter*, *JCAP* **02** (2007) 028 [[hep-ph/0612275](#)].
- [25] A. Belyaev, G. Cacciapaglia, I.P. Ivanov, F. Rojas-Abatte and M. Thomas, *Anatomy of the Inert Two Higgs Doublet Model in the light of the LHC and non-LHC Dark Matter Searches*, *Phys. Rev. D* **97** (2018) 035011 [[1612.00511](#)].
- [26] Y.-L.S. Tsai, C.-T. Lu and V.Q. Tran, *Confronting dark matter co-annihilation of Inert two Higgs Doublet Model with a compressed mass spectrum*, *JHEP* **06** (2020) 033 [[1912.08875](#)].
- [27] F. Wilczek, *Problem of Strong P and T Invariance in the Presence of Instantons*, *Phys. Rev. Lett.* **40** (1978) 279.
- [28] J.E. Kim, *Light Pseudoscalars, Particle Physics and Cosmology*, *Phys. Rept.* **150** (1987) 1.
- [29] A. Celis, J. Fuentes-Martín and H. Serôdio, *Effective Aligned 2HDM with a DFSZ-like invisible axion*, *Phys. Lett. B* **737** (2014) 185 [[1407.0971](#)].
- [30] K. Allison, C.T. Hill and G.G. Ross, *An ultra-weak sector, the strong CP problem and the pseudo-Goldstone dilaton*, *Nucl. Phys. B* **891** (2015) 613 [[1409.4029](#)].
- [31] D. Espriu, F. Mescia and A. Renau, *Axion-Higgs interplay in the two Higgs-doublet model*, *Phys. Rev. D* **92** (2015) 095013 [[1503.02953](#)].
- [32] A. Anuar, A. Biekötter, T. Biekötter, A. Grohsjean, S. Heinemeyer, L. Jeppe et al., *ALP-ine quests at the LHC: hunting axion-like particles via peaks and dips in $t\bar{t}$ production*, [2404.19014](#).
- [33] N. Turok and J. Zadrozny, *Electroweak baryogenesis in the two doublet model*, *Nucl. Phys. B* **358** (1991) 471.
- [34] J.M. Cline, K. Kainulainen and M. Trott, *Electroweak Baryogenesis in Two Higgs Doublet Models and B meson anomalies*, *JHEP* **11** (2011) 089 [[1107.3559](#)].
- [35] K. Fuyuto and E. Senaha, *Sphaleron and critical bubble in the scale invariant two Higgs doublet model*, *Phys. Lett. B* **747** (2015) 152 [[1504.04291](#)].
- [36] G.C. Dorsch, S.J. Huber, T. Konstandin and J.M. No, *A Second Higgs Doublet in the Early Universe: Baryogenesis and Gravitational Waves*, *JCAP* **05** (2017) 052 [[1611.05874](#)].
- [37] P. Basler, L. Biermann, M. Mühlleitner and J. Müller, *Electroweak baryogenesis in the CP-violating two-Higgs doublet model*, *Eur. Phys. J. C* **83** (2023) 57 [[2108.03580](#)].
- [38] K. Enomoto, S. Kanemura and Y. Mura, *New benchmark scenarios of electroweak baryogenesis in aligned two Higgs double models*, *JHEP* **09** (2022) 121 [[2207.00060](#)].
- [39] D. Gonçalves, A. Kaladharan and Y. Wu, *Gravitational waves, bubble profile, and baryon asymmetry in the complex 2HDM*, *Phys. Rev. D* **108** (2023) 075010 [[2307.03224](#)].
- [40] D. Das and I. Saha, *Search for a stable alignment limit in two-Higgs-doublet models*, *Phys. Rev. D* **91** (2015) 095024 [[1503.02135](#)].

- [41] P. Ferreira, H.E. Haber and E. Santos, *Preserving the validity of the Two-Higgs Doublet Model up to the Planck scale*, *Phys. Rev. D* **92** (2015) 033003 [[1505.04001](#)].
- [42] F. Staub, *Reopen parameter regions in Two-Higgs Doublet Models*, *Phys. Lett. B* **776** (2018) 407 [[1705.03677](#)].
- [43] P. Schuh, *Vacuum Stability of Asymptotically Safe Two Higgs Doublet Models*, *Eur. Phys. J. C* **79** (2019) 909 [[1810.07664](#)].
- [44] P.M. Ferreira, L.A. Morrison and S. Profumo, *One-Loop Charge-Breaking Minima in the Two-Higgs Doublet Model*, *JHEP* **04** (2020) 125 [[1910.08662](#)].
- [45] G. Degrandi, S. Di Vita, J. Elias-Miro, J.R. Espinosa, G.F. Giudice, G. Isidori et al., *Higgs mass and vacuum stability in the Standard Model at NNLO*, *JHEP* **08** (2012) 098 [[1205.6497](#)].
- [46] D. Buttazzo, G. Degrandi, P.P. Giardino, G.F. Giudice, F. Sala, A. Salvio et al., *Investigating the near-criticality of the Higgs boson*, *JHEP* **12** (2013) 089 [[1307.3536](#)].
- [47] A.V. Bednyakov, B.A. Kniehl, A.F. Pikelner and O.L. Veretin, *Stability of the Electroweak Vacuum: Gauge Independence and Advanced Precision*, *Phys. Rev. Lett.* **115** (2015) 201802 [[1507.08833](#)].
- [48] S.L. Glashow and S. Weinberg, *Natural Conservation Laws for Neutral Currents*, *Phys. Rev. D* **15** (1977) 1958.
- [49] E.A. Paschos, *Diagonal Neutral Currents*, *Phys. Rev. D* **15** (1977) 1966.
- [50] A. Pich and P. Tuzon, *Yukawa Alignment in the Two-Higgs-Doublet Model*, *Phys. Rev. D* **80** (2009) 091702 [[0908.1554](#)].
- [51] A. Pich, *Flavour constraints on multi-Higgs-doublet models: Yukawa alignment*, *Nucl. Phys. B Proc. Suppl.* **209** (2010) 182 [[1010.5217](#)].
- [52] A. Peñuelas and A. Pich, *Flavour alignment in multi-Higgs-doublet models*, *JHEP* **12** (2017) 084 [[1710.02040](#)].
- [53] G. Abbas, A. Celis, X.-Q. Li, J. Lu and A. Pich, *Flavour-changing top decays in the aligned two-Higgs-doublet model*, *JHEP* **06** (2015) 005 [[1503.06423](#)].
- [54] A. Celis, V. Ilisie and A. Pich, *LHC constraints on two-Higgs doublet models*, *JHEP* **07** (2013) 053 [[1302.4022](#)].
- [55] A. Celis, V. Ilisie and A. Pich, *Towards a general analysis of LHC data within two-Higgs-doublet models*, *JHEP* **12** (2013) 095 [[1310.7941](#)].
- [56] M. Jung, A. Pich and P. Tuzon, *Charged-Higgs phenomenology in the Aligned two-Higgs-doublet model*, *JHEP* **11** (2010) 003 [[1006.0470](#)].
- [57] M. Jung, A. Pich and P. Tuzon, *The $\bar{B} \rightarrow X_s \gamma$ Rate and CP Asymmetry within the Aligned Two-Higgs-Doublet Model*, *Phys. Rev. D* **83** (2011) 074011 [[1011.5154](#)].
- [58] M. Jung, X.-Q. Li and A. Pich, *Exclusive radiative B-meson decays within the aligned two-Higgs-doublet model*, *JHEP* **10** (2012) 063 [[1208.1251](#)].
- [59] P.M. Ferreira, L. Lavoura and J.P. Silva, *Renormalization-group constraints on Yukawa alignment in multi-Higgs-doublet models*, *Phys. Lett. B* **688** (2010) 341 [[1001.2561](#)].
- [60] F.J. Botella, G.C. Branco, A.M. Coutinho, M.N. Rebelo and J.I. Silva-Marcos, *Natural Quasi-Alignment with two Higgs Doublets and RGE Stability*, *Eur. Phys. J. C* **75** (2015) 286 [[1501.07435](#)].

- [61] R.S. Chivukula and H. Georgi, *Composite Technicolor Standard Model*, *Phys. Lett. B* **188** (1987) 99.
- [62] G. D’Ambrosio, G.F. Giudice, G. Isidori and A. Strumia, *Minimal flavor violation: An Effective field theory approach*, *Nucl. Phys. B* **645** (2002) 155 [[hep-ph/0207036](#)].
- [63] A.V. Manohar and M.B. Wise, *Flavor changing neutral currents, an extended scalar sector, and the Higgs production rate at the CERN LHC*, *Phys. Rev. D* **74** (2006) 035009 [[hep-ph/0606172](#)].
- [64] A.J. Buras, M.V. Carlucci, S. Gori and G. Isidori, *Higgs-mediated FCNCs: Natural Flavour Conservation vs. Minimal Flavour Violation*, *JHEP* **10** (2010) 009 [[1005.5310](#)].
- [65] C.B. Braeuninger, A. Ibarra and C. Simonetto, *Radiatively induced flavour violation in the general two-Higgs doublet model with Yukawa alignment*, *Phys. Lett. B* **692** (2010) 189 [[1005.5706](#)].
- [66] J. Bijnens, J. Lu and J. Rathsmann, *Constraining General Two Higgs Doublet Models by the Evolution of Yukawa Couplings*, *JHEP* **05** (2012) 118 [[1111.5760](#)].
- [67] X.-Q. Li, J. Lu and A. Pich, $B_{s,d}^0 \rightarrow \ell^+ \ell^-$ Decays in the Aligned Two-Higgs-Doublet Model, *JHEP* **06** (2014) 022 [[1404.5865](#)].
- [68] S. Gori, H.E. Haber and E. Santos, *High scale flavor alignment in two-Higgs doublet models and its phenomenology*, *JHEP* **06** (2017) 110 [[1703.05873](#)].
- [69] S. Iguro, *Conclusive probe of the charged Higgs solution of $P5'$ and $RD^{(*)}$ discrepancies*, *Phys. Rev. D* **107** (2023) 095004 [[2302.08935](#)].
- [70] T. Mondal, S. Moretti, S. Munir and P. Sanyal, *Electroweak Multi-Higgs Production: A Smoking Gun for the Type-I Two-Higgs-Doublet Model*, *Phys. Rev. Lett.* **131** (2023) 231801 [[2304.07719](#)].
- [71] C. Fu and J. Gao, *Constraint for a light charged Higgs boson and its neutral partners from top quark pairs at the LHC*, *Phys. Rev. D* **108** (2023) 035007 [[2304.07782](#)].
- [72] D. Azevedo, T. Biekötter and P.M. Ferreira, *$2HDM$ interpretations of the CMS diphoton excess at 95 GeV*, *JHEP* **11** (2023) 017 [[2305.19716](#)].
- [73] A. Belyaev, R. Benbrik, M. Boukidi, M. Chakraborti, S. Moretti and S. Semlali, *Explanation of the hints for a 95 GeV Higgs boson within a 2-Higgs Doublet Model*, *JHEP* **05** (2024) 209 [[2306.09029](#)].
- [74] A. Arhrib, S. Moretti, S. Semlali, C.H. Shepherd-Themistocleous, Y. Wang and Q.S. Yan, *Searching for $H \rightarrow hh \rightarrow b\bar{b}\tau\tau$ in the $2HDM$ type-I at the LHC*, *Phys. Rev. D* **109** (2024) 055020 [[2310.02736](#)].
- [75] Y. Ma, A. Arhrib, S. Moretti, S. Semlali, Y. Wang and Q.S. Yan, *Analysis of the $gg \rightarrow H \rightarrow hh \rightarrow 4\tau$ process in the $2HDM$ lepton specific model at the LHC*, [2401.07289](#).
- [76] A. Arhrib, M. Krab and S. Semlali, *Accommodating the LHC charged Higgs boson excess at 130 GeV in the general two-Higgs doublet model*, *J. Phys. G* **51** (2024) 115003 [[2402.03195](#)].
- [77] T. Biekötter, D. Fontes, M. Mühlleitner, J.C. Romão, R. Santos and J.a.P. Silva, *Impact of new experimental data on the $C2HDM$: the strong interdependence between LHC Higgs data and the electron EDM*, *JHEP* **05** (2024) 127 [[2403.02425](#)].
- [78] W. Liu, L. Wang and Y. Zhang, *Direct production of light scalars in the type-I two-*

- Higgs-doublet model at the lifetime frontier of the LHC*, *Phys. Rev. D* **110** (2024) 015016 [2403.16623].
- [79] R. Benrik, M. Boukidi and S. Moretti, *Superposition of CP-Even and CP-Odd Higgs Resonances: Explaining the 95 GeV Excesses within a Two-Higgs Doublet Model*, 2405.02899.
- [80] A. Doff, J.P. Pinheiro and C.A.d.S. Pires, *Exploring solutions to the muon $g-2$ anomaly in a THDM-like model under flavor constraints*, 2405.05839.
- [81] N. Das and N. Ghosh, *Unveiling the CP-odd Higgs in a Generalized 2HDM Model at a Muon Collider*, 2406.18698.
- [82] A. Khanna, S. Moretti and A. Sarkar, *Explaining 95 (or so) GeV Anomalies in the 2-Higgs Doublet Model Type-I*, 2409.02587.
- [83] Y. Dong, K. Wang and J. Zhu, *Probing Type-I 2HDM light Higgs in the top-pair-associated diphoton channel*, 2410.13636.
- [84] S. Banik, G. Coloretti, A. Crivellin and H.E. Haber, *Correlating $A \rightarrow \gamma\gamma$ with EDMs in the 2HDM in light of the diphoton excesses at 95 GeV and 152 GeV*, 2412.00523.
- [85] J. Li, H. Song, S. Su and W. Su, *Charged Higgs Search in 2HDM*, 2412.04572.
- [86] A. Arhrib, S. Moretti, S. Semlali, C.H. Shepherd-Themistocleous, Y. Wang and Q.S. Yan, *Probing a 2HDM Type-I light Higgs state via $H_{SM} \rightarrow hh \rightarrow b\bar{b}\gamma\gamma$ at the LHC*, 2412.06052.
- [87] LEP WORKING GROUP FOR HIGGS BOSON SEARCHES, ALEPH, DELPHI, L3, OPAL collaboration, *Search for the standard model Higgs boson at LEP*, *Phys. Lett. B* **565** (2003) 61 [hep-ex/0306033].
- [88] CMS collaboration, *Search for a standard model-like Higgs boson in the mass range between 70 and 110 GeV in the diphoton final state in proton-proton collisions at $\sqrt{s} = 8$ and 13 TeV*, *Phys. Lett. B* **793** (2019) 320 [1811.08459].
- [89] CMS collaboration, *Search for a standard model-like Higgs boson in the mass range between 70 and 110 GeV in the diphoton final state in proton-proton collisions at $\sqrt{s} = 13$ TeV*, 2405.18149.
- [90] ATLAS collaboration, *Search for diphoton resonances in the 66 to 110 GeV mass range using pp collisions at $\sqrt{s} = 13$ TeV with the ATLAS detector*, 2407.07546.
- [91] A.G. Akeroyd, S. Moretti and J. Hernandez-Sanchez, *Light charged Higgs bosons decaying to charm and bottom quarks in models with two or more Higgs doublets*, *Phys. Rev. D* **85** (2012) 115002 [1203.5769].
- [92] W. Altmannshofer, S. Gori and G.D. Kribs, *A Minimal Flavor Violating 2HDM at the LHC*, *Phys. Rev. D* **86** (2012) 115009 [1210.2465].
- [93] V. Ilisie and A. Pich, *Low-mass fermiophobic charged Higgs phenomenology in two-Higgs-doublet models*, *JHEP* **09** (2014) 089 [1405.6639].
- [94] T. Enomoto and R. Watanabe, *Flavor constraints on the Two Higgs Doublet Models of Z_2 symmetric and aligned types*, *JHEP* **05** (2016) 002 [1511.05066].
- [95] T. Han, S.K. Kang and J. Sayre, *Muon $g - 2$ in the aligned two Higgs doublet model*, *JHEP* **02** (2016) 097 [1511.05162].
- [96] A. Cherchiglia, P. Kneschke, D. Stöckinger and H. Stöckinger-Kim, *The muon magnetic moment in the 2HDM: complete two-loop result*, *JHEP* **01** (2017) 007 [1607.06292].

- [97] A. Cherchiglia, D. Stöckinger and H. Stöckinger-Kim, *Muon $g-2$ in the 2HDM: maximum results and detailed phenomenology*, *Phys. Rev. D* **98** (2018) 035001 [[1711.11567](#)].
- [98] O. Eberhardt, A. Peñuelas Martínez and A. Pich, *Global fits in the Aligned Two-Higgs-Doublet model*, *JHEP* **05** (2021) 005 [[2012.09200](#)].
- [99] A. Karan, V. Miralles and A. Pich, *Updated global fit of the aligned two-Higgs-doublet model with heavy scalars*, *Phys. Rev. D* **109** (2024) 035012 [[2307.15419](#)].
- [100] A. Karan, V. Miralles and A. Pich, *Aligned two Higgs doublet model and the global fits*, *PoS EPS-HEP2023* (2024) 053 [[2312.00514](#)].
- [101] J. De Blas et al., *HEPfit: a code for the combination of indirect and direct constraints on high energy physics models*, *Eur. Phys. J. C* **80** (2020) 456 [[1910.14012](#)].
- [102] A. Karan, A.M. Coutinho, V. Miralles and A. Pich, *Status of the Aligned Two Higgs Doublet Model in the low mass region*, in *42nd International Conference on High Energy Physics*, 9, 2024 [[2409.14934](#)].
- [103] A.M. Coutinho, A. Karan, V. Miralles and A. Pich, *Bayesian analyses of the A2HDM with low-mass scalars*, in *12th Large Hadron Collider Physics Conference*, 10, 2024 [[2410.22274](#)].
- [104] H. Bahl, M. Carena, N.M. Coyle, A. Ireland and C.E.M. Wagner, *New tools for dissecting the general 2HDM*, *JHEP* **03** (2023) 165 [[2210.00024](#)].
- [105] I.P. Ivanov, *Minkowski space structure of the Higgs potential in 2HDM*, *Phys. Rev. D* **75** (2007) 035001 [[hep-ph/0609018](#)].
- [106] I.P. Ivanov and J.P. Silva, *Tree-level metastability bounds for the most general two Higgs doublet model*, *Phys. Rev. D* **92** (2015) 055017 [[1507.05100](#)].
- [107] I.F. Ginzburg and I.P. Ivanov, *Tree-level unitarity constraints in the most general 2HDM*, *Phys. Rev. D* **72** (2005) 115010 [[hep-ph/0508020](#)].
- [108] M.E. Peskin and T. Takeuchi, *A New constraint on a strongly interacting Higgs sector*, *Phys. Rev. Lett.* **65** (1990) 964.
- [109] M.E. Peskin and T. Takeuchi, *Estimation of oblique electroweak corrections*, *Phys. Rev. D* **46** (1992) 381.
- [110] H.E. Haber and D. O’Neil, *Basis-independent methods for the two-Higgs-doublet model III: The CP-conserving limit, custodial symmetry, and the oblique parameters S , T , U* , *Phys. Rev. D* **83** (2011) 055017 [[1011.6188](#)].
- [111] J. de Blas, M. Ciuchini, E. Franco, S. Mishima, M. Pierini, L. Reina et al., *Electroweak precision observables and Higgs-boson signal strengths in the Standard Model and beyond: present and future*, *JHEP* **12** (2016) 135 [[1608.01509](#)].
- [112] J. de Blas, M. Ciuchini, E. Franco, A. Goncalves, S. Mishima, M. Pierini et al., *Global analysis of electroweak data in the Standard Model*, *Phys. Rev. D* **106** (2022) 033003 [[2112.07274](#)].
- [113] J. de Blas, M. Pierini, L. Reina and L. Silvestrini, *Impact of the Recent Measurements of the Top-Quark and W-Boson Masses on Electroweak Precision Fits*, *Phys. Rev. Lett.* **129** (2022) 271801 [[2204.04204](#)].
- [114] H.E. Haber and H.E. Logan, *Radiative corrections to the $Zb\bar{b}$ vertex and constraints on extended Higgs sectors*, *Phys. Rev. D* **62** (2000) 015011 [[hep-ph/9909335](#)].
- [115] G. Degrandi and P. Slavich, *QCD Corrections in two-Higgs-doublet extensions of the Standard Model with Minimal Flavor Violation*, *Phys. Rev. D* **81** (2010) 075001 [[1002.1071](#)].

- [116] CKMFITTER GROUP collaboration, *CP violation and the CKM matrix: Assessing the impact of the asymmetric B factories*, *Eur. Phys. J. C* **41** (2005) 1 [[hep-ph/0406184](#)].
- [117] UTFIT collaboration, *The Unitarity Triangle Fit in the Standard Model and Hadronic Parameters from Lattice QCD: A Reappraisal after the Measurements of Δm_s and $BR(B \rightarrow \tau\nu_\tau)$* , *JHEP* **10** (2006) 081 [[hep-ph/0606167](#)].
- [118] L. Wolfenstein, *Parametrization of the Kobayashi-Maskawa Matrix*, *Phys. Rev. Lett.* **51** (1983) 1945.
- [119] UTFIT collaboration, *The UTfit collaboration report on the status of the unitarity triangle beyond the standard model. I. Model-independent analysis and minimal flavor violation*, *JHEP* **03** (2006) 080 [[hep-ph/0509219](#)].
- [120] Q. Chang, P.-F. Li and X.-Q. Li, *$B_s^0 - \bar{B}_s^0$ mixing within minimal flavor-violating two-Higgs-doublet models*, *Eur. Phys. J. C* **75** (2015) 594 [[1505.03650](#)].
- [121] C. Bobeth, M. Misiak and J. Urban, *Matching conditions for $b \rightarrow s\gamma$ and $b \rightarrow s$ gluon in extensions of the standard model*, *Nucl. Phys. B* **567** (2000) 153 [[hep-ph/9904413](#)].
- [122] M. Misiak and M. Steinhauser, *NNLO QCD corrections to the $\bar{B} \rightarrow X_s\gamma$ matrix elements using interpolation in $m(c)$* , *Nucl. Phys. B* **764** (2007) 62 [[hep-ph/0609241](#)].
- [123] M. Misiak et al., *Estimate of $\mathcal{B}(\bar{B} \rightarrow X_s\gamma)$ at $O(\alpha_s^2)$* , *Phys. Rev. Lett.* **98** (2007) 022002 [[hep-ph/0609232](#)].
- [124] T. Hermann, M. Misiak and M. Steinhauser, *$\bar{B} \rightarrow X_s\gamma$ in the Two Higgs Doublet Model up to Next-to-Next-to-Leading Order in QCD*, *JHEP* **11** (2012) 036 [[1208.2788](#)].
- [125] M. Misiak et al., *Updated NNLO QCD predictions for the weak radiative B-meson decays*, *Phys. Rev. Lett.* **114** (2015) 221801 [[1503.01789](#)].
- [126] M. Misiak, A. Rehman and M. Steinhauser, *NNLO QCD counterterm contributions to $\bar{B} \rightarrow X_{s\gamma}$ for the physical value of m_c* , *Phys. Lett. B* **770** (2017) 431 [[1702.07674](#)].
- [127] M. Misiak, A. Rehman and M. Steinhauser, *Towards $\bar{B} \rightarrow X_s\gamma$ at the NNLO in QCD without interpolation in m_c* , *JHEP* **06** (2020) 175 [[2002.01548](#)].
- [128] P. Arnan, D. Bećirević, F. Mescia and O. Sumensari, *Two Higgs doublet models and $b \rightarrow s$ exclusive decays*, *Eur. Phys. J. C* **77** (2017) 796 [[1703.03426](#)].
- [129] ATLAS collaboration, *A detailed map of Higgs boson interactions by the ATLAS experiment ten years after the discovery*, *Nature* **607** (2022) 52 [[2207.00092](#)].
- [130] CMS collaboration, *A portrait of the Higgs boson by the CMS experiment ten years after the discovery.*, *Nature* **607** (2022) 60 [[2207.00043](#)].
- [131] CMS collaboration, *Search for Higgs Boson Decay to a Charm Quark-Antiquark Pair in Proton-Proton Collisions at $\sqrt{s} = 13$ TeV*, *Phys. Rev. Lett.* **131** (2023) 061801 [[2205.05550](#)].
- [132] ATLAS collaboration, *Direct constraint on the Higgs-charm coupling from a search for Higgs boson decays into charm quarks with the ATLAS detector*, *Eur. Phys. J. C* **82** (2022) 717 [[2201.11428](#)].
- [133] J. Alwall, R. Frederix, S. Frixione, V. Hirschi, F. Maltoni, O. Mattelaer et al., *The automated computation of tree-level and next-to-leading order differential cross sections, and their matching to parton shower simulations*, *JHEP* **07** (2014) 079 [[1405.0301](#)].
- [134] M. Spira, *HIGLU: A program for the calculation of the total Higgs production cross-section at hadron colliders via gluon fusion including QCD corrections*, [hep-ph/9510347](#).

- [135] HDECAY collaboration, *HDECAY: Twenty++ years after*, *Comput. Phys. Commun.* **238** (2019) 214 [[1801.09506](#)].
- [136] LHC HIGGS XS WORKING GROUP, “*BSM Higgs production cross sections at $\sqrt{s} = 8$ TeV (update in CERN Report4 2016)*.” [[twiki.cern.ch](#)].
- [137] LHC HIGGS XS WORKING GROUP, “*BSM Higgs production cross sections at $\sqrt{s} = 13$ TeV (update in CERN Report4 2016)*.” [[twiki.cern.ch](#)].
- [138] S. Iguro, T. Kitahara, M.S. Lang and M. Takeuchi, *Current status of the muon $g-2$ interpretations within two-Higgs-doublet models*, *Phys. Rev. D* **108** (2023) 115012 [[2304.09887](#)].
- [139] A. Freitas, A. von Manteuffel and P.M. Zerwas, *Slepton production at e^+e^- and e^-e^- linear colliders*, *Eur. Phys. J. C* **34** (2004) 487 [[hep-ph/0310182](#)].
- [140] LHC SUSY CROSS SECTION WORKING GROUP, “*Slepton/stau-pair cross sections computed at NLO+NLL and NLO+NNLL*.” [[twiki.cern.ch](#)].
- [141] J. Fiaschi and M. Klasen, *Slepton pair production at the LHC in NLO+NLL with resummation-improved parton densities*, *JHEP* **03** (2018) 094 [[1801.10357](#)].
- [142] B. Fuks, M. Klasen, D.R. Lamprea and M. Rothering, *Revisiting slepton pair production at the Large Hadron Collider*, *JHEP* **01** (2014) 168 [[1310.2621](#)].
- [143] A. Caldwell, D. Kollar and K. Kroninger, *BAT: The Bayesian Analysis Toolkit*, *Comput. Phys. Commun.* **180** (2009) 2197 [[0808.2552](#)].
- [144] J. De Blas, G. Durieux, C. Grojean, J. Gu and A. Paul, *On the future of Higgs, electroweak and diboson measurements at lepton colliders*, *JHEP* **12** (2019) 117 [[1907.04311](#)].
- [145] G. Durieux, A. Irlles, V. Miralles, A. Peñuelas, R. Pöschl, M. Perelló et al., *The electro-weak couplings of the top and bottom quarks — Global fit and future prospects*, *JHEP* **12** (2019) 98 [[1907.10619](#)].
- [146] A.M. Coutinho, A. Crivellin and C.A. Manzari, *Global Fit to Modified Neutrino Couplings and the Cabibbo-Angle Anomaly*, *Phys. Rev. Lett.* **125** (2020) 071802 [[1912.08823](#)].
- [147] L. Alasfar, A. Azatov, J. de Blas, A. Paul and M. Valli, *B anomalies under the lens of electroweak precision*, *JHEP* **12** (2020) 016 [[2007.04400](#)].
- [148] A. Crivellin, F. Kirk, C.A. Manzari and M. Montull, *Global Electroweak Fit and Vector-Like Leptons in Light of the Cabibbo Angle Anomaly*, *JHEP* **12** (2020) 166 [[2008.01113](#)].
- [149] T. Husek, K. Monsalvez-Pozo and J. Portoles, *Lepton-flavour violation in hadronic tau decays and $\mu - \tau$ conversion in nuclei*, *JHEP* **01** (2021) 059 [[2009.10428](#)].
- [150] A. Crivellin, M. Hoferichter and C.A. Manzari, *Fermi Constant from Muon Decay Versus Electroweak Fits and Cabibbo-Kobayashi-Maskawa Unitarity*, *Phys. Rev. Lett.* **127** (2021) 071801 [[2102.02825](#)].
- [151] L. Darmé, M. Fedele, K. Kowalska and E.M. Sessolo, *Flavour anomalies and the muon $g - 2$ from feebly interacting particles*, *JHEP* **03** (2022) 085 [[2106.12582](#)].
- [152] V. Miralles, M. Miralles López, M. Moreno Llácer, A. Peñuelas, M. Perelló and M. Vos, *The top quark electro-weak couplings after LHC Run 2*, *JHEP* **02** (2022) 032 [[2107.13917](#)].
- [153] A. Paul and M. Valli, *Violation of custodial symmetry from W-boson mass measurements*, *Phys. Rev. D* **106** (2022) 013008 [[2204.05267](#)].

- [154] V. Miralles, Y. Peters, E. Vryonidou and J.K. Winter, *Sensitivity to CP-violating effective couplings in the top-Higgs sector*, [2412.10309](#).
- [155] V. Cacchio, D. Chowdhury, O. Eberhardt and C.W. Murphy, *Next-to-leading order unitarity fits in Two-Higgs-Doublet models with soft \mathbb{Z}_2 breaking*, *JHEP* **11** (2016) 026 [[1609.01290](#)].
- [156] C.-W. Chiang, G. Cottin and O. Eberhardt, *Global fits in the Georgi-Machacek model*, *Phys. Rev. D* **99** (2019) 015001 [[1807.10660](#)].
- [157] L. Cheng, O. Eberhardt and C.W. Murphy, *Novel theoretical constraints for color-octet scalar models*, *Chin. Phys. C* **43** (2019) 093101 [[1808.05824](#)].
- [158] O. Eberhardt, V. Miralles and A. Pich, *Constraints on coloured scalars from global fits*, *JHEP* **10** (2021) 123 [[2106.12235](#)].
- [159] T.-K. Chen, C.-W. Chiang, C.-T. Huang and B.-Q. Lu, *Updated constraints on the Georgi-Machacek model and its electroweak phase transition and associated gravitational waves*, *Phys. Rev. D* **106** (2022) 055019 [[2205.02064](#)].
- [160] Y. Cheng, X.-G. He, F. Huang, J. Sun and Z.-P. Xing, *Electroweak precision tests for triplet scalars*, *Nucl. Phys. B* **989** (2023) 116118 [[2208.06760](#)].
- [161] T.-K. Chen, C.-W. Chiang and K. Yagyu, *CP violation in a model with Higgs triplets*, *JHEP* **06** (2023) 069 [[2303.09294](#)].
- [162] G. D'Agostini, *Bayesian reasoning in high-energy physics: Principles and applications*, in *CERN Yellow Reports: Monographs*, CERN-99-03, CERN-YELLOW-99-03 (1999).
- [163] M. Ciuchini, G. D'Agostini, E. Franco, V. Lubicz, G. Martinelli, F. Parodi et al., *2000 CKM triangle analysis: A Critical review with updated experimental inputs and theoretical parameters*, *JHEP* **07** (2001) 013 [[hep-ph/0012308](#)].
- [164] T. Ando, *Bayesian predictive information criterion for the evaluation of hierarchical bayesian and empirical bayes models*, *Biometrika* **94** (2007) 443.
- [165] T. Ando, *Predictive bayesian model selection*, *Am. J. Math.-S* **31** (2011) 13.
- [166] A. Gelman, J. Hwang and A. Vehtari, *Understanding predictive information criteria for bayesian models*, [1307.5928](#).
- [167] H. Jeffreys, *The Theory of Probability*, 3rd ed. (Oxford Classic Texts in the Physical Sciences), Oxford University Press, Oxford, UK (1998).
- [168] R.E. Kass and A.E. Raftery, *Bayes factors*, *J. Am. Stat. Assoc.* **90** (1995) 773.
- [169] A. Bartl, K. Hidaka, K. Hohenwarter-Sodek, T. Kernreiter, W. Majerotto and W. Porod, *Test of lepton flavor violation at LHC*, *Eur. Phys. J. C* **46** (2006) 783 [[hep-ph/0510074](#)].
- [170] CMS collaboration, *Search for direct pair production of supersymmetric partners of τ leptons in the final state with two hadronically decaying τ leptons and missing transverse momentum in proton-proton collisions at $\sqrt{s} = 13$ TeV*, *Phys. Rev. D* **108** (2023) 012011 [[2207.02254](#)].
- [171] V. Ilisie, *New Barr-Zee contributions to $(\mathbf{g} - 2)_\mu$ in two-Higgs-doublet models*, *JHEP* **04** (2015) 077 [[1502.04199](#)].
- [172] B.e. Lautrup, A. Peterman and E. de Rafael, *Recent developments in the comparison between theory and experiments in quantum electrodynamics*, *Phys. Rept.* **3** (1972) 193.
- [173] J.P. Leveille, *The Second Order Weak Correction to $(G-2)$ of the Muon in Arbitrary Gauge Models*, *Nucl. Phys. B* **137** (1978) 63.

- [174] A. Czarnecki, B. Krause and W.J. Marciano, *Electroweak Fermion loop contributions to the muon anomalous magnetic moment*, *Phys. Rev. D* **52** (1995) R2619 [[hep-ph/9506256](#)].
- [175] A. Dedes and H.E. Haber, *Can the Higgs sector contribute significantly to the muon anomalous magnetic moment?*, *JHEP* **05** (2001) 006 [[hep-ph/0102297](#)].
- [176] D. Chang, W.-F. Chang, C.-H. Chou and W.-Y. Keung, *Large two loop contributions to $g-2$ from a generic pseudoscalar boson*, *Phys. Rev. D* **63** (2001) 091301 [[hep-ph/0009292](#)].
- [177] K.-m. Cheung, C.-H. Chou and O.C.W. Kong, *Muon anomalous magnetic moment, two Higgs doublet model, and supersymmetry*, *Phys. Rev. D* **64** (2001) 111301 [[hep-ph/0103183](#)].
- [178] K. Cheung and O.C.W. Kong, *Can the two Higgs doublet model survive the constraint from the muon anomalous magnetic moment as suggested?*, *Phys. Rev. D* **68** (2003) 053003 [[hep-ph/0302111](#)].
- [179] P. Athron, C. Balazs, A. Cherchiglia, D.H.J. Jacob, D. Stöckinger, H. Stöckinger-Kim et al., *Two-loop prediction of the anomalous magnetic moment of the muon in the Two-Higgs Doublet Model with GM2Calc 2*, *Eur. Phys. J. C* **82** (2022) 229 [[2110.13238](#)].
- [180] T. Aoyama et al., *The anomalous magnetic moment of the muon in the Standard Model*, *Phys. Rept.* **887** (2020) 1 [[2006.04822](#)].
- [181] M. Davier, A. Hoecker, A.-M. Lutz, B. Malaescu and Z. Zhang, *Tensions in $e^+e^- \rightarrow \pi^+\pi^-(\gamma)$ measurements: the new landscape of data-driven hadronic vacuum polarization predictions for the muon $g-2$* , *Eur. Phys. J. C* **84** (2024) 721 [[2312.02053](#)].
- [182] P. Masjuan, A. Miranda and P. Roig, *τ data-driven evaluation of Euclidean windows for the hadronic vacuum polarization*, *Phys. Lett. B* **850** (2024) 138492 [[2305.20005](#)].
- [183] A. Boccaletti et al., *High precision calculation of the hadronic vacuum polarisation contribution to the muon anomaly*, [2407.10913](#).
- [184] CMD-3 collaboration, *Measurement of the $e^+e^- \rightarrow \pi^+\pi^-$ cross section from threshold to 1.2 GeV with the CMD-3 detector*, *Phys. Rev. D* **109** (2024) 112002 [[2302.08834](#)].
- [185] CMD-3 collaboration, *Measurement of the Pion Form Factor with CMD-3 Detector and its Implication to the Hadronic Contribution to Muon ($g-2$)*, *Phys. Rev. Lett.* **132** (2024) 231903 [[2309.12910](#)].
- [186] MUON G-2 collaboration, *Measurement of the Positive Muon Anomalous Magnetic Moment to 0.20 ppm*, *Phys. Rev. Lett.* **131** (2023) 161802 [[2308.06230](#)].
- [187] MUON G-2 collaboration, *Detailed report on the measurement of the positive muon anomalous magnetic moment to 0.20 ppm*, *Phys. Rev. D* **110** (2024) 032009 [[2402.15410](#)].
- [188] L. Wang and X.-F. Han, *A light pseudoscalar of 2HDM confronted with muon $g-2$ and experimental constraints*, *JHEP* **05** (2015) 039 [[1412.4874](#)].
- [189] T. Abe, R. Sato and K. Yagyu, *Lepton-specific two Higgs doublet model as a solution of muon $g-2$ anomaly*, *JHEP* **07** (2015) 064 [[1504.07059](#)].
- [190] P. Athron, C. Balázs, D.H.J. Jacob, W. Kotlarski, D. Stöckinger and H. Stöckinger-Kim, *New physics explanations of a_μ in light of the FNAL muon $g-2$ measurement*, *JHEP* **09** (2021) 080 [[2104.03691](#)].
- [191] A. Jueid, J. Kim, S. Lee and J. Song, *Type-X two-Higgs-doublet model in light of the muon $g-2$: Confronting Higgs boson and collider data*, *Phys. Rev. D* **104** (2021) 095008 [[2104.10175](#)].

- [192] A. Dey, J. Lahiri and B. Mukhopadhyaya, *Muon $g-2$ and a type-X two-Higgs-doublet scenario: Some studies in high-scale validity*, *Phys. Rev. D* **106** (2022) 055023 [2106.01449].
- [193] F.J. Botella, F. Cornet-Gomez, C. Miró and M. Nebot, *Muon and electron $g-2$ anomalies in a flavor conserving 2HDM with an oblique view on the CDF M_W value*, *Eur. Phys. J. C* **82** (2022) 915 [2205.01115].
- [194] Y. Afik, P.S. Bhupal Dev and A. Thapa, *Hints of a new leptophilic Higgs sector?*, *Phys. Rev. D* **109** (2024) 015003 [2305.19314].
- [195] Z. Fodor, A. Gerardin, L. Lellouch, K.K. Szabo, B.C. Toth and C. Zimmermann, *Hadronic light-by-light scattering contribution to the anomalous magnetic moment of the muon at the physical pion mass*, [2411.11719](#).
- [196] CMS collaboration, *Search for a Low-Mass Pseudoscalar Higgs Boson Produced in Association with a $b\bar{b}$ Pair in pp Collisions at $\sqrt{s} = 8$ TeV*, *Phys. Lett. B* **758** (2016) 296 [1511.03610].
- [197] CMS collaboration, *Search for light bosons in decays of the 125 GeV Higgs boson in proton-proton collisions at $\sqrt{s} = 8$ TeV*, *JHEP* **10** (2017) 076 [1701.02032].
- [198] CMS collaboration, *Search for a light pseudoscalar Higgs boson produced in association with bottom quarks in pp collisions at $\sqrt{s} = 8$ TeV*, *JHEP* **11** (2017) 010 [1707.07283].
- [199] CMS collaboration, *Search for an exotic decay of the Higgs boson to a pair of light pseudoscalars in the final state of two muons and two τ leptons in proton-proton collisions at $\sqrt{s} = 13$ TeV*, *JHEP* **11** (2018) 018 [1805.04865].
- [200] CMS collaboration, *Search for exotic decays of the Higgs boson to a pair of pseudoscalars in the $\mu\mu b\bar{b}$ and $\tau\tau b\bar{b}$ final states*, *Eur. Phys. J. C* **84** (2024) 493 [2402.13358].
- [201] CMS collaboration, *Search for a low-mass $\tau^+\tau^-$ resonance in association with a bottom quark in proton-proton collisions at $\sqrt{s} = 13$ TeV*, *JHEP* **05** (2019) 210 [1903.10228].
- [202] CMS collaboration, *Search for light pseudoscalar boson pairs produced from decays of the 125 GeV Higgs boson in final states with two muons and two nearby tracks in pp collisions at $\sqrt{s} = 13$ TeV*, *Phys. Lett. B* **800** (2020) 135087 [1907.07235].
- [203] CMS collaboration, *Search for low-mass dilepton resonances in Higgs boson decays to four-lepton final states in proton-proton collisions at $\sqrt{s} = 13$ TeV*, *Eur. Phys. J. C* **82** (2022) 290 [2111.01299].
- [204] CMS collaboration, *Search for an exotic decay of the Higgs boson into a Z boson and a pseudoscalar particle in proton-proton collisions at $\sqrt{s} = 13$ TeV*, *Phys. Lett. B* **852** (2024) 138582 [2311.00130].
- [205] CMS collaboration, *Search for the exotic decay of the Higgs boson into two light pseudoscalars with four photons in the final state in proton-proton collisions at $\sqrt{s} = 13$ TeV*, *JHEP* **07** (2023) 148 [2208.01469].
- [206] CMS collaboration, *Search for the decay of the Higgs boson to a pair of light pseudoscalar bosons in the final state with four bottom quarks in proton-proton collisions at $\sqrt{s} = 13$ TeV*, *JHEP* **06** (2024) 097 [2403.10341].
- [207] CMS collaboration, *Search for a scalar or pseudoscalar dilepton resonance produced in association with a massive vector boson or top quark-antiquark pair in multilepton events at $\sqrt{s} = 13$ TeV*, *Phys. Rev. D* **110** (2024) 012013 [2402.11098].

- [208] ATLAS collaboration, *Search for Higgs bosons decaying to aa in the $\mu\mu\tau\tau$ final state in pp collisions at $\sqrt{s} = 8$ TeV with the ATLAS experiment*, *Phys. Rev. D* **92** (2015) 052002 [[1505.01609](#)].
- [209] ATLAS collaboration, *Search for new phenomena in events with at least three photons collected in pp collisions at $\sqrt{s} = 8$ TeV with the ATLAS detector*, *Eur. Phys. J. C* **76** (2016) 210 [[1509.05051](#)].
- [210] ATLAS collaboration, *Search for Higgs boson decays into pairs of light (pseudo)scalar particles in the $\gamma\gamma jj$ final state in pp collisions at $\sqrt{s} = 13$ TeV with the ATLAS detector*, *Phys. Lett. B* **782** (2018) 750 [[1803.11145](#)].
- [211] ATLAS collaboration, *Search for the Higgs boson produced in association with a vector boson and decaying into two spin-zero particles in the $H \rightarrow aa \rightarrow 4b$ channel in pp collisions at $\sqrt{s} = 13$ TeV with the ATLAS detector*, *JHEP* **10** (2018) 031 [[1806.07355](#)].
- [212] ATLAS collaboration, *Search for Higgs boson decays into a pair of light bosons in the $b\bar{b}\mu\mu$ final state in pp collision at $\sqrt{s} = 13$ TeV with the ATLAS detector*, *Phys. Lett. B* **790** (2019) 1 [[1807.00539](#)].
- [213] ATLAS collaboration, *Search for Higgs boson decays into two new low-mass spin-0 particles in the $4b$ channel with the ATLAS detector using pp collisions at $\sqrt{s} = 13$ TeV*, *Phys. Rev. D* **102** (2020) 112006 [[2005.12236](#)].
- [214] ATLAS collaboration, *Search for Higgs boson decays into a pair of pseudoscalar particles in the $b\bar{b}\mu\mu$ final state with the ATLAS detector in pp collisions at $\sqrt{s} = 13$ TeV*, *Phys. Rev. D* **105** (2022) 012006 [[2110.00313](#)].
- [215] ATLAS collaboration, *Search for Higgs bosons decaying into new spin-0 or spin-1 particles in four-lepton final states with the ATLAS detector with 139 fb^{-1} of pp collision data at $\sqrt{s} = 13$ TeV*, *JHEP* **03** (2022) 041 [[2110.13673](#)].
- [216] ATLAS collaboration, *Search for a new pseudoscalar decaying into a pair of muons in events with a top-quark pair at $\sqrt{s} = 13$ TeV with the ATLAS detector*, *Phys. Rev. D* **108** (2023) 092007 [[2304.14247](#)].
- [217] ATLAS collaboration, *Search for decays of the Higgs boson into a pair of pseudoscalar particles decaying into $b\bar{b}\tau^+\tau^-$ using pp collisions at $\sqrt{s} = 13$ TeV with the ATLAS detector*, *Phys. Rev. D* **110** (2024) 052013 [[2407.01335](#)].
- [218] ATLAS collaboration, *Search for short- and long-lived axion-like particles in $H \rightarrow aa \rightarrow 4\gamma$ decays with the ATLAS experiment at the LHC*, *Eur. Phys. J. C* **84** (2024) 742 [[2312.03306](#)].
- [219] ATLAS collaboration, *Search for a light CP-odd Higgs boson decaying into a pair of τ -leptons in proton-proton collisions at $\sqrt{s} = 13$ TeV with the ATLAS detector*, [2409.20381](#).
- [220] LEP HIGGS WORKING GROUP, ALEPH, DELPHI, L3, OPAL collaboration, *Searches for Higgs bosons decaying into photons: Preliminary combined results using LEP data collected at energies up to 209-GeV*, in *2001 Europhysics Conference on High Energy Physics*, 7, 2001 [[hep-ex/0107035](#)].
- [221] ALEPH, DELPHI, L3, OPAL, LEP WORKING GROUP FOR HIGGS BOSON SEARCHES collaboration, *Search for neutral MSSM Higgs bosons at LEP*, *Eur. Phys. J. C* **47** (2006) 547 [[hep-ex/0602042](#)].
- [222] CMS collaboration, *Search for resonant pair production of Higgs bosons decaying to two*

- bottom quark–antiquark pairs in proton–proton collisions at 8 TeV, *Phys. Lett. B* **749** (2015) 560 [1503.04114].
- [223] CMS collaboration, Search for two Higgs bosons in final states containing two photons and two bottom quarks in proton–proton collisions at 8 TeV, *Phys. Rev. D* **94** (2016) 052012 [1603.06896].
- [224] CMS collaboration, Searches for a heavy scalar boson H decaying to a pair of 125 GeV Higgs bosons hh or for a heavy pseudoscalar boson A decaying to Zh , in the final states with $h \rightarrow \tau\tau$, *Phys. Lett. B* **755** (2016) 217 [1510.01181].
- [225] CMS collaboration, Search for Higgs boson pair production in the $b\bar{b}\tau\tau$ final state in proton–proton collisions at $\sqrt{s} = 8$ TeV, *Phys. Rev. D* **96** (2017) 072004 [1707.00350].
- [226] CMS collaboration, Search for a pseudoscalar boson decaying into a Z boson and the 125 GeV Higgs boson in $\ell^+\ell^-\bar{b}b$ final states, *Phys. Lett. B* **748** (2015) 221 [1504.04710].
- [227] CMS collaboration, Search for neutral resonances decaying into a Z boson and a pair of b jets or τ leptons, *Phys. Lett. B* **759** (2016) 369 [1603.02991].
- [228] CMS collaboration, Search for resonant pair production of Higgs bosons decaying to bottom quark–antiquark pairs in proton–proton collisions at 13 TeV, *JHEP* **08** (2018) 152 [1806.03548].
- [229] CMS collaboration, Search for resonant pair production of Higgs bosons in the $b\bar{b}b\bar{b}$ final state using large-area jets in proton–proton collisions at $\sqrt{s} = 13$ TeV, **2407.13872**.
- [230] CMS collaboration, Search for Higgs boson pairs decaying to WW^*WW^* , $WW^*\tau\tau$, and $\tau\tau\tau\tau$ in proton–proton collisions at $\sqrt{s} = 13$ TeV, *JHEP* **07** (2023) 095 [2206.10268].
- [231] CMS collaboration, Search for a new resonance decaying into two spin-0 bosons in a final state with two photons and two bottom quarks in proton–proton collisions at $\sqrt{s} = 13$ TeV, *JHEP* **05** (2024) 316 [2310.01643].
- [232] CMS collaboration, Search for Higgs boson pair production in events with two bottom quarks and two tau leptons in proton–proton collisions at $\sqrt{s} = 13$ TeV, *Phys. Lett. B* **778** (2018) 101 [1707.02909].
- [233] CMS collaboration, Search for heavy resonances decaying into two Higgs bosons or into a Higgs boson and a W or Z boson in proton–proton collisions at 13 TeV, *JHEP* **01** (2019) 051 [1808.01365].
- [234] CMS collaboration, Search for resonant and nonresonant Higgs boson pair production in the $b\bar{b}\ell\nu\ell\nu$ final state in proton–proton collisions at $\sqrt{s} = 13$ TeV, *JHEP* **01** (2018) 054 [1708.04188].
- [235] CMS collaboration, Search for resonances decaying to a pair of Higgs bosons in the $b\bar{b}q\bar{q}'\ell\nu$ final state in proton–proton collisions at $\sqrt{s} = 13$ TeV, *JHEP* **10** (2019) 125 [1904.04193].
- [236] CMS collaboration, Search for resonant pair production of Higgs bosons in the $b\bar{b}ZZ$ channel in proton–proton collisions at $\sqrt{s} = 13$ TeV, *Phys. Rev. D* **102** (2020) 032003 [2006.06391].
- [237] CMS collaboration, Search for heavy resonances decaying to a pair of Lorentz-boosted Higgs bosons in final states with leptons and a bottom quark pair at $\sqrt{s} = 13$ TeV, *JHEP* **05** (2022) 005 [2112.03161].
- [238] CMS collaboration, Search for Higgs boson pair production in the $b\bar{b}W^+W^-$ decay mode in proton–proton collisions at $\sqrt{s} = 13$ TeV, *JHEP* **07** (2024) 293 [2403.09430].

- [239] CMS collaboration, *Search for a heavy pseudoscalar boson decaying to a Z and a Higgs boson at $\sqrt{s} = 13$ TeV*, *Eur. Phys. J. C* **79** (2019) 564 [[1903.00941](#)].
- [240] CMS collaboration, *Search for heavy resonances decaying into a vector boson and a Higgs boson in final states with charged leptons, neutrinos and b quarks at $\sqrt{s} = 13$ TeV*, *JHEP* **11** (2018) 172 [[1807.02826](#)].
- [241] CMS collaboration, *Search for a heavy pseudoscalar Higgs boson decaying into a 125 GeV Higgs boson and a Z boson in final states with two tau and two light leptons at $\sqrt{s} = 13$ TeV*, *JHEP* **03** (2020) 065 [[1910.11634](#)].
- [242] ATLAS collaboration, *Searches for Higgs boson pair production in the $hh \rightarrow bb\tau\tau, \gamma\gamma WW^*, \gamma\gamma bb, bbbb$ channels with the ATLAS detector*, *Phys. Rev. D* **92** (2015) 092004 [[1509.04670](#)].
- [243] ATLAS collaboration, *Search for a CP-odd Higgs boson decaying to Zh in pp collisions at $\sqrt{s} = 8$ TeV with the ATLAS detector*, *Phys. Lett. B* **744** (2015) 163 [[1502.04478](#)].
- [244] ATLAS collaboration, *Search for resonant pair production of Higgs bosons in the $b\bar{b}b\bar{b}$ final state using pp collisions at $\sqrt{s} = 13$ TeV with the ATLAS detector*, *Phys. Rev. D* **105** (2022) 092002 [[2202.07288](#)].
- [245] ATLAS collaboration, *Search for Higgs boson pair production in the two bottom quarks plus two photons final state in pp collisions at $\sqrt{s} = 13$ TeV with the ATLAS detector*, *Phys. Rev. D* **106** (2022) 052001 [[2112.11876](#)].
- [246] ATLAS collaboration, *Search for resonant and non-resonant Higgs boson pair production in the $b\bar{b}\tau^+\tau^-$ decay channel using 13 TeV pp collision data from the ATLAS detector*, *JHEP* **07** (2023) 040 [[2209.10910](#)].
- [247] ATLAS collaboration, *Reconstruction and identification of boosted di- τ systems in a search for Higgs boson pairs using 13 TeV proton-proton collision data in ATLAS*, *JHEP* **11** (2020) 163 [[2007.14811](#)].
- [248] ATLAS collaboration, *Search for Higgs boson pair production in the $b\bar{b}WW^*$ decay mode at $\sqrt{s} = 13$ TeV with the ATLAS detector*, *JHEP* **04** (2019) 092 [[1811.04671](#)].
- [249] ATLAS collaboration, *Search for Higgs boson pair production in the $\gamma\gamma WW^*$ channel using pp collision data recorded at $\sqrt{s} = 13$ TeV with the ATLAS detector*, *Eur. Phys. J. C* **78** (2018) 1007 [[1807.08567](#)].
- [250] ATLAS collaboration, *Search for heavy resonances decaying into a Z or W boson and a Higgs boson in final states with leptons and b-jets in 139 fb^{-1} of pp collisions at $\sqrt{s} = 13$ TeV with the ATLAS detector*, *JHEP* **06** (2023) 016 [[2207.00230](#)].
- [251] ATLAS collaboration, *Search for a heavy Higgs boson decaying into a Z boson and another heavy Higgs boson in the $\ell\bar{\ell}bb$ and $\ell\bar{\ell}WW$ final states in pp collisions at $\sqrt{s} = 13$ TeV with the ATLAS detector*, *Eur. Phys. J. C* **81** (2021) 396 [[2011.05639](#)].
- [252] CMS collaboration, *Search for scalar resonances in the 200–1200 GeV mass range decaying into a Z and a photon in pp collisions at $\sqrt{s} = 8$ TeV*, *CMS-PAS-HIG-16-014* (2016) .
- [253] CMS collaboration, *Search for a Higgs boson in the mass range from 145 to 1000 GeV decaying to a pair of W or Z bosons*, *JHEP* **10** (2015) 144 [[1504.00936](#)].
- [254] CMS collaboration, *Search for new physics in high-mass diphoton events from proton-proton collisions at $\sqrt{s} = 13$ TeV*, *JHEP* **08** (2024) 215 [[2405.09320](#)].

- [255] CMS collaboration, *Search for $Z\gamma$ resonances using leptonic and hadronic final states in proton-proton collisions at $\sqrt{s} = 13$ TeV*, *JHEP* **09** (2018) 148 [[1712.03143](#)].
- [256] CMS collaboration, *Search for a new scalar resonance decaying to a pair of Z bosons in proton-proton collisions at $\sqrt{s} = 13$ TeV*, *JHEP* **06** (2018) 127 [[1804.01939](#)].
- [257] CMS collaboration, *Search for a heavy resonance decaying into a Z boson and a vector boson in the $\nu\bar{\nu}q\bar{q}$ final state*, *JHEP* **07** (2018) 075 [[1803.03838](#)].
- [258] CMS collaboration, *Search for a heavy Higgs boson decaying to a pair of W bosons in proton-proton collisions at $\sqrt{s} = 13$ TeV*, *JHEP* **03** (2020) 034 [[1912.01594](#)].
- [259] CMS collaboration, *Search for a heavy resonance decaying to a pair of vector bosons in the lepton plus merged jet final state at $\sqrt{s} = 13$ TeV*, *JHEP* **05** (2018) 088 [[1802.09407](#)].
- [260] CMS collaboration, *Search for heavy resonances decaying to WW , WZ , or WH boson pairs in the lepton plus merged jet final state in proton-proton collisions at $\sqrt{s} = 13$ TeV*, *Phys. Rev. D* **105** (2022) 032008 [[2109.06055](#)].
- [261] CMS collaboration, *Search for high mass Higgs to WW with fully leptonic decays using 2015 data*, *CMS-PAS-HIG-16-023* (2016) .
- [262] ATLAS collaboration, *Search for Scalar Diphoton Resonances in the Mass Range 65 – 600 GeV with the ATLAS Detector in pp Collision Data at $\sqrt{s} = 8$ TeV*, *Phys. Rev. Lett.* **113** (2014) 171801 [[1407.6583](#)].
- [263] ATLAS collaboration, *Search for new resonances in $W\gamma$ and $Z\gamma$ final states in pp collisions at $\sqrt{s} = 8$ TeV with the ATLAS detector*, *Phys. Lett. B* **738** (2014) 428 [[1407.8150](#)].
- [264] ATLAS collaboration, *Search for an additional, heavy Higgs boson in the $H \rightarrow ZZ$ decay channel at $\sqrt{s} = 8$ TeV in pp collision data with the ATLAS detector*, *Eur. Phys. J. C* **76** (2016) 45 [[1507.05930](#)].
- [265] ATLAS collaboration, *Search for a high-mass Higgs boson decaying to a W boson pair in pp collisions at $\sqrt{s} = 8$ TeV with the ATLAS detector*, *JHEP* **01** (2016) 032 [[1509.00389](#)].
- [266] ATLAS collaboration, *Search for resonances decaying into photon pairs in 139 fb^{-1} of pp collisions at $\sqrt{s}=13$ TeV with the ATLAS detector*, *Phys. Lett. B* **822** (2021) 136651 [[2102.13405](#)].
- [267] ATLAS collaboration, *Search for the $Z\gamma$ decay mode of new high-mass resonances in pp collisions at $s=13$ TeV with the ATLAS detector*, *Phys. Lett. B* **848** (2024) 138394 [[2309.04364](#)].
- [268] ATLAS collaboration, *Search for high-mass $W\gamma$ and $Z\gamma$ resonances using hadronic W/Z boson decays from 139 fb^{-1} of pp collisions at $\sqrt{s} = 13$ TeV with the ATLAS detector*, *JHEP* **07** (2023) 125 [[2304.11962](#)].
- [269] ATLAS collaboration, *Search for heavy resonances decaying into a pair of Z bosons in the $\ell^+\ell^-\ell'^+\ell'^-$ and $\ell^+\ell^-\nu\bar{\nu}$ final states using 139 fb^{-1} of proton-proton collisions at $\sqrt{s} = 13$ TeV with the ATLAS detector*, *Eur. Phys. J. C* **81** (2021) 332 [[2009.14791](#)].
- [270] ATLAS collaboration, *Searches for heavy ZZ and ZW resonances in the $\ell\ell q\bar{q}$ and $\nu\nu q\bar{q}$ final states in pp collisions at $\sqrt{s} = 13$ TeV with the ATLAS detector*, *JHEP* **03** (2018) 009 [[1708.09638](#)].
- [271] ATLAS collaboration, *Search for heavy resonances in the decay channel $W^+W^- \rightarrow e\nu_e\mu\nu_\mu$ in pp collisions at $\sqrt{s} = 13$ TeV using 139 fb^{-1} of data with the ATLAS detector*, *ATLAS-CONF-2022-066* (2022) .

- [272] ATLAS collaboration, *Search for WW/WZ resonance production in $lvqq$ final states in pp collisions at $\sqrt{s} = 13$ TeV with the ATLAS detector*, *JHEP* **03** (2018) 042 [[1710.07235](#)].
- [273] ATLAS collaboration, *Search for diboson resonances with boson-tagged jets in pp collisions at $\sqrt{s} = 13$ TeV with the ATLAS detector*, *Phys. Lett. B* **777** (2018) 91 [[1708.04445](#)].
- [274] ATLAS collaboration, *Search for heavy diboson resonances in semileptonic final states in pp collisions at $\sqrt{s} = 13$ TeV with the ATLAS detector*, *Eur. Phys. J. C* **80** (2020) 1165 [[2004.14636](#)].
- [275] CMS collaboration, *Search for neutral MSSM Higgs bosons decaying into a pair of bottom quarks*, *JHEP* **11** (2015) 071 [[1506.08329](#)].
- [276] CMS collaboration, *Search for narrow resonances in the b-tagged dijet mass spectrum in proton-proton collisions at $\sqrt{s} = 8$ TeV*, *Phys. Rev. Lett.* **120** (2018) 201801 [[1802.06149](#)].
- [277] CMS collaboration, *Search for neutral MSSM Higgs bosons decaying to $\mu^+\mu^-$ in pp collisions at $\sqrt{s} = 7$ and 8 TeV*, *Phys. Lett. B* **752** (2016) 221 [[1508.01437](#)].
- [278] CMS collaboration, *Search for additional neutral Higgs bosons decaying to a pair of tau leptons in pp collisions at $\sqrt{s} = 7$ and 8 TeV*, *CMS-PAS-HIG-14-029* (2015) .
- [279] CMS collaboration, *Search for production of four top quarks in final states with same-sign or multiple leptons in proton-proton collisions at $\sqrt{s} = 13$ TeV*, *Eur. Phys. J. C* **80** (2020) 75 [[1908.06463](#)].
- [280] CMS collaboration, *Search for a narrow heavy decaying to bottom quark pairs in the 13 TeV data sample*, *CMS-PAS-HIG-16-025* (2016) .
- [281] CMS collaboration, *Search for low-mass resonances decaying into bottom quark-antiquark pairs in proton-proton collisions at $\sqrt{s} = 13$ TeV*, *Phys. Rev. D* **99** (2019) 012005 [[1810.11822](#)].
- [282] CMS collaboration, *Search for beyond the standard model Higgs bosons decaying into a $b\bar{b}$ pair in pp collisions at $\sqrt{s} = 13$ TeV*, *JHEP* **08** (2018) 113 [[1805.12191](#)].
- [283] CMS collaboration, *Search for MSSM Higgs bosons decaying to $\mu^+\mu^-$ in proton-proton collisions at $\sqrt{s} = 13$ TeV*, *Phys. Lett. B* **798** (2019) 134992 [[1907.03152](#)].
- [284] CMS collaboration, *Searches for additional Higgs bosons and for vector leptoquarks in $\tau\tau$ final states in proton-proton collisions at $\sqrt{s} = 13$ TeV*, *JHEP* **07** (2023) 073 [[2208.02717](#)].
- [285] ATLAS collaboration, *Search for neutral Higgs bosons of the minimal supersymmetric standard model in pp collisions at $\sqrt{s} = 8$ TeV with the ATLAS detector*, *JHEP* **11** (2014) 056 [[1409.6064](#)].
- [286] ATLAS collaboration, *Search for pair production of up-type vector-like quarks and for four-top-quark events in final states with multiple b-jets with the ATLAS detector*, *JHEP* **07** (2018) 089 [[1803.09678](#)].
- [287] ATLAS collaboration, *Search for $t\bar{t}H/A \rightarrow t\bar{t}\bar{t}$ production in the multilepton final state in proton-proton collisions at $\sqrt{s} = 13$ TeV with the ATLAS detector*, *JHEP* **07** (2023) 203 [[2211.01136](#)].
- [288] ATLAS collaboration, *Search for resonances in the mass distribution of jet pairs with one or two jets identified as b-jets in proton-proton collisions at $\sqrt{s} = 13$ TeV with the ATLAS detector*, *Phys. Rev. D* **98** (2018) 032016 [[1805.09299](#)].

- [289] ATLAS collaboration, *Search for heavy neutral Higgs bosons produced in association with b -quarks and decaying into b -quarks at $\sqrt{s} = 13$ TeV with the ATLAS detector*, *Phys. Rev. D* **102** (2020) 032004 [[1907.02749](#)].
- [290] ATLAS collaboration, *Search for scalar resonances decaying into $\mu^+\mu^-$ in events with and without b -tagged jets produced in proton-proton collisions at $\sqrt{s} = 13$ TeV with the ATLAS detector*, *JHEP* **07** (2019) 117 [[1901.08144](#)].
- [291] ATLAS collaboration, *Search for heavy Higgs bosons decaying into two tau leptons with the ATLAS detector using pp collisions at $\sqrt{s} = 13$ TeV*, *Phys. Rev. Lett.* **125** (2020) 051801 [[2002.12223](#)].
- [292] CMS collaboration, *Search for a charged Higgs boson in pp collisions at $\sqrt{s} = 8$ TeV*, *JHEP* **11** (2015) 018 [[1508.07774](#)].
- [293] CMS collaboration, *Search for a light charged Higgs boson decaying to $c\bar{s}$ in pp collisions at $\sqrt{s} = 8$ TeV*, *JHEP* **12** (2015) 178 [[1510.04252](#)].
- [294] CMS collaboration, *Search for a charged Higgs boson decaying to charm and bottom quarks in proton-proton collisions at $\sqrt{s} = 8$ TeV*, *JHEP* **11** (2018) 115 [[1808.06575](#)].
- [295] CMS collaboration, *Search for a light charged Higgs boson decaying to a W boson and a CP -odd Higgs boson in final states with $e\mu\mu$ or $\mu\mu\mu$ in proton-proton collisions at $\sqrt{s} = 13$ TeV*, *Phys. Rev. Lett.* **123** (2019) 131802 [[1905.07453](#)].
- [296] CMS collaboration, *Search for a light charged Higgs boson in the $H^\pm \rightarrow cs$ channel in proton-proton collisions at $\sqrt{s} = 13$ TeV*, *Phys. Rev. D* **102** (2020) 072001 [[2005.08900](#)].
- [297] ATLAS collaboration, *Search for charged Higgs bosons decaying via $H^\pm \rightarrow \tau^\pm\nu$ in fully hadronic final states using pp collision data at $\sqrt{s} = 8$ TeV with the ATLAS detector*, *JHEP* **03** (2015) 088 [[1412.6663](#)].
- [298] ATLAS collaboration, *Search for a light charged Higgs boson in $t \rightarrow H^\pm b$ decays, with $H^\pm \rightarrow cb$, in the lepton+jets final state in proton-proton collisions at $\sqrt{s} = 13$ TeV with the ATLAS detector*, *JHEP* **09** (2023) 004 [[2302.11739](#)].
- [299] ATLAS collaboration, *Search for a light charged Higgs boson in $t \rightarrow H^\pm b$ decays, with $H^\pm \rightarrow cs$, in pp collisions at $\sqrt{s} = 13$ TeV with the ATLAS detector*, [2407.10096](#).
- [300] ALEPH, DELPHI, L3, OPAL, LEP collaboration, *Search for Charged Higgs bosons: Combined Results Using LEP Data*, *Eur. Phys. J. C* **73** (2013) 2463 [[1301.6065](#)].
- [301] OPAL collaboration, *Search for Charged Higgs Bosons in e^+e^- Collisions at $\sqrt{s} = 189-209$ GeV*, *Eur. Phys. J. C* **72** (2012) 2076 [[0812.0267](#)].
- [302] CMS collaboration, *Search for charged Higgs bosons in the $H^\pm \rightarrow \tau^\pm\nu_\tau$ decay channel in proton-proton collisions at $\sqrt{s} = 13$ TeV*, *JHEP* **07** (2019) 142 [[1903.04560](#)].
- [303] CMS collaboration, *Search for charged Higgs bosons decaying into a top and a bottom quark in the all-jet final state of pp collisions at $\sqrt{s} = 13$ TeV*, *JHEP* **07** (2020) 126 [[2001.07763](#)].
- [304] ATLAS collaboration, *Search for charged Higgs bosons in the $H^\pm \rightarrow tb$ decay channel in pp collisions at $\sqrt{s} = 8$ TeV using the ATLAS detector*, *JHEP* **03** (2016) 127 [[1512.03704](#)].
- [305] ATLAS collaboration, *Search for charged Higgs bosons decaying via $H^\pm \rightarrow \tau^\pm\nu_\tau$ in the τ +jets and τ +lepton final states with 36 fb^{-1} of pp collision data recorded at $\sqrt{s} = 13$ TeV with the ATLAS experiment*, *JHEP* **09** (2018) 139 [[1807.07915](#)].

- [306] ATLAS collaboration, *Search for charged Higgs bosons decaying into a top quark and a bottom quark at $\sqrt{s} = 13$ TeV with the ATLAS detector*, *JHEP* **06** (2021) 145 [[2102.10076](#)].
- [307] ATLAS collaboration, *Combination of searches for invisible decays of the Higgs boson using 139 fb^{-1} of proton-proton collision data at $\sqrt{s} = 13$ TeV collected with the ATLAS experiment*, *Phys. Lett. B* **842** (2023) 137963 [[2301.10731](#)].
- [308] CMS collaboration, *Precision measurement of the Z boson invisible width in pp collisions at $\sqrt{s} = 13$ TeV*, *Phys. Lett. B* **842** (2023) 137563 [[2206.07110](#)].
- [309] ALEPH collaboration, *Measurement of W pair production in e^+e^- collisions at 183-GeV*, *Phys. Lett. B* **453** (1999) 107 [[hep-ex/9903053](#)].
- [310] CMS collaboration, *Measurement of the ratio $\mathcal{B}(t \rightarrow Wb)/\mathcal{B}(t \rightarrow Wq)$ in pp collisions at $\sqrt{s} = 8$ TeV*, *Phys. Lett. B* **736** (2014) 33 [[1404.2292](#)].
- [311] PARTICLE DATA GROUP collaboration, *Review of particle physics*, *Phys. Rev. D* **110** (2024) 030001.
- [312] LEP SUSY WORKING GROUP, M. Berggren et al., “*Combined LEP Selectron/Smuon/Stau Results, 183-208 GeV.*” [[lepsusy.web.cern.ch](#)].
- [313] ATLAS collaboration, *Search for direct pair production of sleptons and charginos decaying to two leptons and neutralinos with mass splittings near the W-boson mass in $\sqrt{s} = 13$ TeV pp collisions with the ATLAS detector*, *JHEP* **06** (2023) 031 [[2209.13935](#)].
- [314] ATLAS collaboration, *Search for direct stau production in events with two hadronic τ -leptons in $\sqrt{s} = 13$ TeV pp collisions with the ATLAS detector*, *Phys. Rev. D* **101** (2020) 032009 [[1911.06660](#)].
- [315] CMS collaboration, *Combined search for electroweak production of winos, binos, higgsinos, and sleptons in proton-proton collisions at $\sqrt{s} = 13$ TeV*, *Phys. Rev. D* **109** (2024) 112001 [[2402.01888](#)].